広島大学学位論文

Studies on novel molecular mechanisms in zebrafish fin regeneration

（ゼブラフィッシュ尾びれ再生における

新規分子メカニズムの研究）

2015 年

広島大学大学院理学研究科

生物科学専攻

廣瀬健太朗

目次

1. 主論文

Studies on novel molecular mechanisms in zebrafish fin regeneration
(ゼブラフィッシュ尾びれ再生における新規分子メカニズムの研究)

廣瀬 健太朗

2. 公表論文

(1) Transient reduction of 5-methylcytosine and 5-hydroxymethylcytosine
is associated with active DNA demethylation during regeneration of
zebrafish fin.
Kentaro Hirose, Nobuyoshi Shimoda, and Yutaka Kikuchi,
Epigenetics. 2013; 8(9): 899–906.

(2) Mechanistic target of rapamycin complex 1 signaling regulates cell
proliferation, cell survival, and differentiation in regenerating zebrafish
fins
Kentaro Hirose, Taishi Shiomi, Shunya Hozumi, and Yutaka Kikuchi
BMC Dev Biol. 2014; 14(1): 42.

主論文

Studies on novel molecular mechanisms in zebrafish fin regeneration

Kentaro Hirose

Department of Biological Science,

Graduate School of Science,

Hiroshima University

2015

Contents

Publication of the thesis

(1) **Transient reduction of 5-methylcytosine and 5-hydroxymethylcytosine is associated with active DNA demethylation during regeneration of zebrafish fin.**
Kentaro Hirose, Nobuyoshi Shimoda, and Yutaka Kikuchi,
Epigenetics. 2013; 8(9): 899–906.

(2) **Mechanistic target of rapamycin complex 1 signaling regulates cell proliferation, cell survival, and differentiation in regenerating zebrafish fins**
Kentaro Hirose, Taishi Shiomi, Shunya Hozumi, and Yutaka Kikuchi
BMC Dev Biol. 2014; 14(1): 42.

Chapter 1. General introduction

General introduction

Mammals exhibit a limited ability for organ regeneration, whereas various non-mammalian vertebrates such as teleosts and urodele amphibians show an outstanding regenerative ability. For example, mice can only regenerate an injured heart during the neonatal period [1], whereas zebrafish can regenerate one throughout their lifetime [2]. Therefore, if the mechanisms of regeneration in non-mammalian vertebrates can be elucidated, application to human medicine may be discover. The zebrafish is powerful for analysis of regeneration mechanisms, because these fish can completely and repeatedly regenerate their organs after injury, including fins, heart, spinal cord, retina, liver, pancreas, and brain after injury [3,4]. Among their organs, the caudal fin is a useful tool for analysis regeneration mechanisms, because it can easy be accessed and manipulated.

The caudal fin of adult zebrafish consists of fin-rays and an epidermis that covers and connects the fin-rays. Each fin-ray is composed of multiple cell types, including fibroblast-like cells, osteoblasts, endothelial cells, melanocytes, and neural axons. The regeneration processes that occur in the fin-rays can be classified into three stages: pre-blastema formation, blastema formation, and regenerative outgrowth. Fin-ray regeneration is usually completed within two weeks (figure) [5-7]. The details are as follows:

1. Pre-blastema formation: ~24 hours post amputation (hpa)

   Following fin amputation, epidermal cells migrate to cover the wound within 12 hpa [7]. The intra-ray cells dedifferentiate and migrate toward the amputation plane [7].

2. Blastema formation: ~48 hpa

   From 18 hpa to 24 hpa, dedifferentiated cells begin to proliferate and, as a result, a population of these cells, named the blastema, forms underneath the wound epidermis by 48 hpa [5].

3. Regenerative outgrowth: 48 hpa~

   Regenerative outgrowth is caused by proliferation and re-differentiation of the blastema, and fin regeneration is complete after approximately two weeks [7].

It has already been reported that the regeneration process requires many growth factors, immune systems factors, epigenetic modifications, and intercellular signaling pathways [7-10]. However, the detailed mechanism of regeneration still remains to be completely elucidated. In this study, I elucidated two novel molecular mechanisms that are involved in caudal fin regeneration in zebrafish.

The purpose of Chapter 2 was to investigate changes in 5-methylcytosine (5mC) and 5-hydroxymethycytosine (5hmC) levels during fin regeneration. The epigenetic markers 5mC and 5hmC have been implicated in many biological processes, such as embryonic development, carcinogenesis, and diseases via regulation of gene expression, genomic imprinting, and genome stability [11-13]. However, few reports have been published regarding levels of 5mC and 5hmC during regeneration in non-mammalian vertebrates. Therefore, I analyzed the spatiotemporal distributions of 5mC and 5hmC by using immunohistochemical and dot blot analyses, and found that the levels of 5mC and 5hmC are transiently reduced in dedifferentiated cells, independent of DNA replication. In addition, I detected expression of active DNA demethylation- and DNA repair-related genes during fin regeneration. In this chapter, I show that the transient reduction of 5mC and 5hmC in dedifferentiated cells is associated with active DNA demethylation during zebrafish fin regeneration.

The purpose of Chapter 3 was to reveal the function of the mechanistic target of rapamycin complex1 (mTORC1) signaling pathway during fin regeneration. Although mTORC1 has been implicated in functions of multicellular processes including cell growth and metabolism [14,15], its functions in non-mammalian vertebrate regeneration remained unknown. Therefore, I analyzed the activation and function of mTORC1 signaling by using immunohistochemical analysis, and mTORC1 inhibitiors, respectively. I found that mTORC1 was activated throughout the regenerating fin, and that it regulated cell proliferation, expression of blastema markers, cell survival, and re-differentiation of osteoblasts at various stages of fin regeneration. Furthermore, I determined that the IGFR-PI3K and Wnt pathways regulate mTORC1 activation. In this chapter, I show the distribution of mTORC1 activation, the functions of mTORC1 during various stages of fin regeneration and the upstream signals of mTORC1.

Finally, in Chapter 4, I discuss how two novel molecular mechanisms are involved in zebrafish fin regeneration.

References

1. Porrello ER, Mahmoud AI, Simpson E, Hill JA, Richardson JA, Olson EN, Sadek HA. Science. Transient regenerative potential of the neonatal mouse heart. Science. 2011 ,331(6020):1078-80

2. Poss KD, Wilson LG, Keating MT. Heart regeneration in zebrafish. Science. 2002, 298(5601):2188-90.

3. Nechiporuk A, Keating MT: A proliferation gradient between proximal and msxb-expressing distal blastema directs zebrafish fin regeneration. Development 2002, 129(11):2607-2617.

4. Akimenko MA, Marí-Beffa M, Becerra J, Géraudie J: Old questions, new tools, and some answers to the mystery of fin regeneration. Dev Dyn 2003, 226(2):190-201.

5. Nechiporuk A, Keating MT: A proliferation gradient between proximal and msxb-expressing distal blastema directs zebrafish fin regeneration. Development 2002, 129(11):2607-2617.

6. Akimenko MA, Marí-Beffa M, Becerra J, Géraudie J: Old questions, new tools, and some answers to the mystery of fin regeneration. Dev Dyn 2003, 226(2):190-201.

7. Poss KD, Keating MT, Nechiporuk A: Tales of regeneration in zebrafish. Dev Dyn 2003, 226(2):202-210.

8. Tal TL, Franzosa JA, Tanguay RL. Molecular signaling networks that choreograph epimorphic fin regeneration in zebrafish - a mini-review. Gerontology. 2010;56(2):231-40.A

9. Petrie TA, Strand NS, Tsung-Yang C, Rabinowitz JS, Moon RT. Macrophages modulate adult zebrafish tail fin regeneration. Development. 2014, 141(13):2581-91

10. Katsuyama T[1], Paro R. Epigenetic reprogramming during tissue regeneration. FEBS Lett, 2011, 585(11):1617-24.

11. Wu SC, Zhang Y. Active DNA demethylation: many roads lead to Rome. Nat Rev Mol Cell Biol 2010; 11:607-20.

12. Cedar H, Bergman Y. Programming of DNA methylation patterns. Annu Rev Biochem 2012; 81:97-117.

13. Franchini DM, Schmitz KM, Petersen-Mahrt SK. 5-Methylcytosine DNA Demethylation: More Than Losing a Methyl Group. Annu Rev Genet 2012.

14. Li J, Kim SG, Blenis J: Rapamycin: One Drug, Many Effects. Cell Metab 2014, 19(3):373-379.

15. Laplante M, Sabatini DM: mTOR signaling in growth control and disease. Cell 2012, 149(2):274-293.
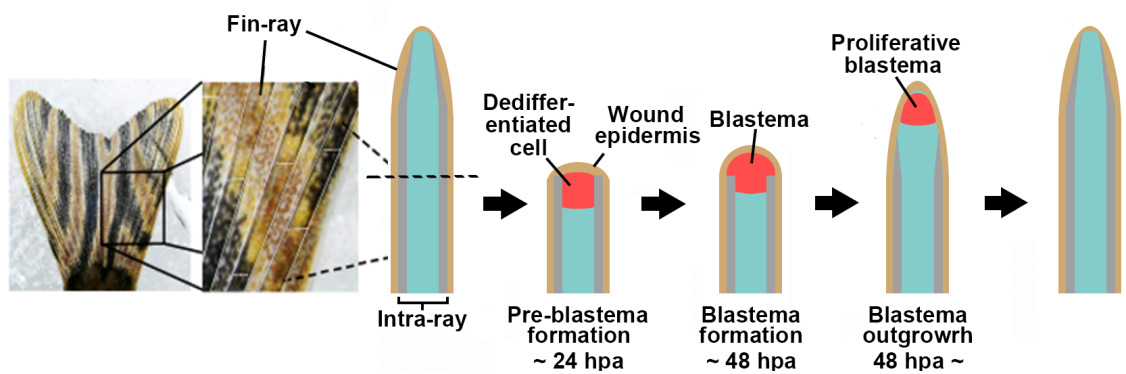
Figure. The process of zebrafish fin regeneration

Following amputation, epidermal cells migrate to cover the injury and form the wound epidermis. The inta-ray cells dedifferentiate and migrate toward the under wound epidermis until 24 hpa. The Dedifferentiated cells begin to proliferate and form blastema. Formed blastema repeat to proliferate and re-differentiate, as a result, regenerative outgrowth is occurred. Finally, regeneration is complicated for two weeks.

Chapter 2. Transient reduction of 5-methylcytosine and 5-hydroxymethylcytosine is associated with active DNA demethylation during regeneration of zebrafish fin.

Abstract

Although dedifferentiation, transformation of differentiated cells into progenitor cells, is a critical step in the regeneration of amphibians and fish, the molecular mechanisms underlying this process, including epigenetic changes, remain unclear. Dot blot assays and immunohistochemical analyses revealed that, during regeneration of zebrafish fin, the levels of 5-methylcytosine (5mC) and 5-hydroxymethylcytosine (5hmC) are transiently reduced in blastema cells and cells adjacent to the amputation plane at 30 h post-amputation (hpa), and the level of 5mC, but not 5hmC, is almost restored by 72 hpa. We observed that the dedifferentiated cells showed reduced levels of 5mC and 5hmC independent of cell proliferation by 24 hpa. Furthermore, expressions of the proposed demethylation- and DNA repair-related genes were detected during fin regeneration. Taken together, our findings illustrate that the transient reduction of 5mC and 5hmC in dedifferentiated cells is associated with active demethylation during regeneration of zebrafish fin.

Introduction

In animals, cytosine methylation (5-methylcytosine; 5mC) of genomic DNA is an epigenetic mechanism that is implicated in many biological processes such as regulation of gene expression, cellular proliferation, differentiation, pluripotency, oncogenesis, and genomic imprinting [1-3]. The methylation pattern of genomic DNA is established and maintained by the activity of *de novo* and maintenance methyltransferases, respectively [4,5]. Conversely, 5mC is reverted to cytosine through active demethylation, which is well studied in the reprogramming of the paternal pronuclei in fertilized mouse zygotes and in primordial germ cells during mouse embryonic development [1,3]. However, the mechanisms underlying active demethylation are still unclear [1,3]. Recently, numerous and intense studies have shown that active demethylation is regulated by many enzymes including cytidine deaminase (activation-induced deaminase, AID; apolipoprotein B mRNA-editing enzymes, Apobec), G/T mismatch DNA glycosylase (thymine-DNA glycosylase, TDG; methyl CpG binding domain protein 4, MBD4), methylcytosine dioxygenase (ten-eleven translocation, Tet), and DNA repair-related factors such as poly-(ADP-ribose) polymerase (PARP), uracil DNA glycosylase (UNG), and MutS homolog 2/6 (MSH2/6) [1,3,6,7]. In one of these proposed demethylation pathways, 5mC is modified to 5-hydroxymethylcytosine (5hmC) by Tet proteins, and 5hmC is though to be a novel epigenetic mark for gene regulation [8-10].

Zebrafish is a common animal model and has been used to study regeneration of various organs [11-13]. It is well known that dedifferentiation processes such as the loss of molecular markers for differentiated cells, re-expression of molecular markers for progenitor cells, and restart of cell proliferation occur during regeneration in amphibians and zebrafish [13,14]. Although epigenetic modifications are thought to be critical for the dedifferentiation processes in regeneration [15,16], only 2 studies concerning DNA methylation have been reported thus far. These studies showed that the demethylation of a *Xenopus elongation factor 1-a* (*ef1-a*):*EGFP* transgene in transgenic zebrafish (Tg(*ef1-a:EGFP*)) was observed during fin regeneration [17] and that the *sonic hedgehog* gene expression is correlated with the methylation status of the limb-specific *sonic hedgehog* enhancer in *Xenopus* limb regeneration [18]. However, despite these findings, the status and changes of DNA methylation during regeneration

remain largely unknown.

It has been already reported that during early zebrafish development, the dynamic change of the 5mC or 5hmC distribution was observed in zebrafish embryos and larvae [19-22]. However, the distribution of these epigenetic markers during regeneration has not yet been reported. In this study, we analyzed the spatial and temporal changes of 5mC or 5hmC distribution during zebrafish fin regeneration by using dot blot assays and immunohistochemical analyses.

Results

Spatial and temporal distributions of 5mC and 5hmC during fin regeneration

Because knowledge concerning changes in 5mC or 5hmC level and zebrafish fin regeneration is limited, we evaluated the level of 2 epigenetic marks by using dot blot assays in genomic DNA from amputated fins at 0, 30, and 72 hours post-amputation (hpa). The levels of both 5mC and 5hmC at 30 hpa were significantly lower than those at 0 hpa (see Fig. S1). These results suggest that both epigenetic marks are transiently down-regulated in the early stages of fin regeneration. To explore the spatial distribution of 5mC or 5hmC in the fin regenerates, we next performed immunohistochemical staining by using longitudinal sections of the regenerates (Fig. S2). The intra-ray cells, which show the same level of 5mC or 5hmC fluorescent signal, were uniformly distributed within the 500 mm proximal region to the amputation plane at 0 hpa (Fig. 1A). The 5mC or 5hmC fluorescent level was not changed between before amputation and at 0 hpa (Fig. S3). However, we found that both signals start to reduce in the cells adjacent to the amputation plane at around 12 hpa and these reduced signals are evident by 18 hpa (Fig. S4). At 30 hpa, the fluorescent signals of 5mC and 5hmC in the blastema and intra-ray cells within the 150 mm proximal region to the amputation plane were markedly lower than those in the intra-ray cells at 0 hpa (Fig. 1B, D, E). In the blastema cells, the level of 5mC signal was almost restored at 72 hpa (Fig. 1C, D), whereas the level of 5hmC signal at 72 hpa remained lower than that at 0 hpa (Fig. 1C, E). The 5hmC level was gradually up-regulated by the end of regeneration (14 days post amputation (dpa)) (Fig. S5 and data not shown). Interestingly, high levels of 5mC and 5hmC in the epidermal and inter-ray cells are maintained before and after regeneration by immunohistochemical staining (Fig. 1, Fig. S2, Fig. S4, and data not shown). Because these epidermal and inter-ray cells are included in dot blot assays, the relative 5mC or 5hmC level at 30 hpa observed in the dot blot assays could be higher than that observed in the immunohistochemical analyses (Fig. 1 and Fig. S1).

5mC and 5hmC are reduced in the dedifferentiated blastema cells and proliferation cells

To test whether the intra-ray cells, which show reduced levels of 5mC and 5hmC, are

dedifferentiated cells, we examined the expression of *Xenopus ef1-a:EGFP* transgene by using Tg(*ef1-a:EGFP*) [23] and proliferating cell nuclear antigen (PCNA), which is detected throughout the G1, S, and G2/M phases [24]. Expression of *Xenopus ef1-a:EGFP* transgene was not detected before amputation (Fig. S6), and this transgene was re-expressed in some of the blastema cells and cells adjacent to the amputation plane (Fig. 2A and Fig. S6G, K), indicating that theses EGFP$^+$ cells are dedifferentiation cells. Immunohistochemical staining using a 5mC antibody revealed that these EGFP$^+$ cells show reduced level of 5mC at 24 hpa (Fig. 2A, B). Moreover, majority of the blastema cells showing low-5hmC are PCNA positive at 24 hpa (Fig. 2C-E). These results suggest that the blastema cells are dedifferentiated cells and are re-entering the cell cycle.

The reduction of 5mC and 5hmC is associated with Active demethylation

In addition, these results suggest that demethylation during fin regeneration may be a replication-dependent process (i.e., passive demethylation). To investigate this possibility, we examined the relationship between the demethylation and cell proliferation in the blastema cells and cells adjacent to the amputation plane by analyzing the bromodeoxyuridine (BrdU) incorporation. Most blastema cells and cells adjacent to the amputation plane, which show reduced level of 5mC or 5hmC, did not incorporate the BrdU until 24 hpa (Fig. 2F-I), suggesting that these cells are still in the G1 phase, and not in the S or G2/M phase, and the active demethylation processes lead to the reduction of both 5mC and 5hmC in the blastema cells and cells adjacent to the amputation plane until 24 hpa.

Demethylation- and DNA repair-related genes express in fin regeneration

Recently, numerous and intense investigations have shown that active demethylation is regulated by specific enzymes, including members of the cytidine deaminase family, G/T mismatch DNA glycosylase, and methylcytosine dioxygenase, as well as DNA repair factors [1,3,6,7]. Moreover, a recent paper showed that many demethylation-related genes are expressed during regeneration of zebrafish retina [25]. Therefore, we next examined the expressions of 11 demethylation- and DNA repair-related genes (*growth arrest and DNA damage 45ba; gadd45ba, gadd45bb, gadd45g, aid, apobec2a, apobec2b, tdg, mbd4, tet2, tet3*, and *parp1*) during fin

regeneration by using quantitative real-time PCR (qPCR). Expressions of *aid* and *apobec2a* were not detected before and after fin amputation (data not shown). Although the relative expressions of *gadd45ba*, *gadd45bb*, *apobec2b*, *tdg*, *mbd4*, *tet2*, *tet3*, and *parp1* were not markedly up-regulated after fin amputation, the relative expression of *gadd45g* was significantly up-regulated at 18 and 30 hpa (Fig. 3).   These data also suggest that down-regulation of 5mC and 5hmC is associated with active demethylation during fin regeneration.

Discussion

A previous report revealed that, after fin amputation, mesenchymal tissue is disorganized and intra-ray cells, which are proximally located (up to 160 mm away from the amputation plane), migrate to the amputation plane [11,12,26].   In this study, we showed that the intra-ray cells, which exhibit reduced level of 5mC or 5hmC, are not observed within 160 mm from the amputation plane at 0 hpa (Fig. 1).   Our results, combined with the findings of a previous report, suggest that the levels of 5mC and 5hmC in the intra-ray cells are reduced during or after migration to the amputation plane.

Our results indicated that although majority of the blastema cells are PCNA positive, almost all of them did not incorporate the BrdU by 24 hpa.   There are 2 possible explanations for these results: (1) these blastema cells are still in the G1 phase and (2) the DNA repair process is active in the blastema cells at 24 hpa, because PCNA is a component of the base excision repair process and is thought to be active in demethylation pathways [3].   PCNA possibly functions in DNA repair process of active demethylation in the blastema cells at 24 hpa.   In either case, our results suggest that the reduction of 5mC or 5hmC is thought to be an epigenetic marker for dedifferentiation.

The main finding of our study is that the levels of both 5mC and 5hmC are transiently reduced in the dedifferentiated blastema cells and the cells adjacent to the amputation plane by active demethylation.   This is the first report to suggest that global and active DNA demethylation in dedifferentiated cells occurs during regeneration.   Previous studies have reported that the global and active DNA demethylation is also observed in reprogramming process of the paternal pronuclei in fertilized mouse zygotes and primordial germ cells [1-3].   Moreover, numerous studies have shown that DNA demethylation influences gene transcription, DNA replication, etc., and that 5hmC is involved in the regulation of gene expression [1-10].   Therefore, the reduction of 5mC and 5hmC during fin regeneration may lead to dedifferentiation, in which genes for fin regeneration are re-expressed and the cell cycle is restarted. Further studies will be necessary to elucidate the relationship between dedifferentiation and DNA demethylation during zebrafish fin regeneration.

The results of qPCR revealed that although *gadd45g* expression is significantly

up-regulated at 18 and 30 hpa, the expression level of eight demethylation- and DNA repair-related genes (*gadd45ba*, *gadd45bb*, *apobec2b*, *tdg*, *mbd4*, *tet2*, *tet3*, and *parp1*) are maintained or down-regulated after amputation (Fig. 3).   Gadd45 family proteins have been implicated in their functions as an adaptor protein in DNA demethylation and DNA repair process, due to the lack of obvious enzymatic activity.   Recent studies reported that making complex of Gadd45 with Aid, Apobec, Mbd4, TDG, or factors for nucleotide excision repair promotes DNA demethylation and DAN repair [6,7]. Therefore, it is possible that the up-regulation of zebrafish *gadd45g* is critical for DNA demethylation and DNA repair processes during fin regeneration.   In addition, although Tet has also been implicated in DNA demethylation through the conversion from 5mC to 5hmC, the 5mC level was reduced simultaneously with the 5hmC level. A possible explanation for this result is that the conversion from 5mC to 5hmC may be too fast to detect the differences between the levels of 5mC and 5hmC by immunohistochemical staining.   Knockdown experiments of the demethylation- or DNA repair-related genes are needed for the functional analyses of these genes to validate their role on the changes of 5mC or 5hmC level during fin regeneration.

Based on our results, we propose a model for the spatial and temporal DNA methylation profile during zebrafish fin regeneration (Fig. 4).   The levels of both 5mC and 5hmC in the dedifferentiated blastema cells and cells adjacent to the amputation plane are transiently reduced from 12 hpa, independent of cell proliferation by 24 hpa. It is thought that after 24 hpa, the dedifferentiation of blastema cells start to proliferate and the proliferation leads to regenerative outgrowth.   In addition, we found that DNA demethylation- and repair-related genes are expressed during fin regeneration and especially expression of *gadd45g* is increased after fin regeneration.   These results suggest that transient reduction of 5mC and 5hmC is associated with active DNA demethylation during zebrafish fin regeneration.

Materials and Methods

Ethics statement

All animal experiments were conducted according to relevant national and international guidelines 'Act on Welfare and Management of Animals' (Ministry of Environment of Japan). Ethics approval from the Hiroshima University Animal Research Committee (HuARC) was not sought since this law does not mandate protection of fish.

Zebrafish husbandry and fin amputation

Adult zebrafish and zebrafish embryos were maintained under a 14-h day/ 10-h night cycle at 28.5 ˚C. Transgenic zebrafish XIG8A (Tg(*ef1-a:EGFP*)) [23] was obtained from National Institute of Genetics (Shizuoka, Japan).

Adult wild-type 3-6-month-old zebrafish (AB/Tüebingen strain) were used for all experiments. For caudal fin amputation, fish were anesthetized using tricaine, and approximately two-third of fins were cut with a blade. After fin amputation, these fish were allowed to regenerate in the aquarium until defined time points at 28.5 ˚C.

Dot blot assays

Dot blot assays were performed as described previously [27,28]. Immediately after fin amputation (0 hpa), the fins were cut within 1000 mm from the amputation plane, and at 30 and 72 hpa, the blastema regions were cut. For the dot blot assays, 3, 6, and 3 amputated fins at 0, 30, and 72 hpa, respectively were used, and the experiments for 5mC and 5hmC were repeated 6 times, respectively. After lysis of the fins or blastema, genomic DNA was purified using the Gentra Puregene Tissue Kit (Qiagen) according to the manufacturer's instructions. The concentration of purified genomic DNA in each regeneration stages was measured using a NanoDrop 1000 (Thermo Fisher Scientific). The genomic DNA (6.25, 25, or 100 ng) was loaded onto a nylon membrane (Amersham Hybond N+, GE Healthcare Life Sciences) and was crosslinked using the Ultraviolet crosslinker CL-1000 (UVP Inc.). The following primary antibodies were used: anti-5mC mouse monoclonal antibody at 1:500 (Calbiochem) and anti-5hmC rabbit polyclonal antibody at 1:1000 (Active motif). The following secondary antibodies were used: anti-rabbit IgG-horseradish peroxidase

(HRP) antibody at 1:250000 (Santa Cruz Biotechnology) and anti-mouse IgG-HRP antibody at 1:250000 (GE Healthcare).   The signal of 5mC or 5hmC was exposed to X-ray film by using the ECL Prime Western Blotting Detection System (GE Healthcare Life Sciences) according to the manufacturer's instructions.   The intensities of these signals were scanned and the images were analyzed using the ImageJ software (NIH). *p*-values were calculated by using Student's *t* test.

Immunohistochemistry

Immediately after fin amputation (0 hpa), the fins were cut within 1000 mm from the amputation plane, and at 24, 30, and 72 hpa, the blastema regions were cut.   The amputated fins were fixed in 4% paraformaldehyde in 0.1 M phosphate-buffered saline (PBS) overnight at 4 ˚C.   After fixation, the fins were treated with PBS containing 30% sucrose overnight, and were embedded with Tissue-Tek O.C.T. compound (Sakura Finetek).   The embedded fins were frozen and sectioned to 14 mm thickness by using a Leica CM3050S.   The sections were dehydrated through a methanol/PBS-0.1% Tween (PBS) series, incubated in 2 N HCl for 30 min at 28.5 ˚C, and then neutralized with PBS for 5 min.   After neutralization, the sections were blocked with PBDT (PBS, 1% DMSO, and 0.5% Tween20) containing 5% sheep serum for 3 h at room temperature and then incubated in PBDT with primary antibody/antibodies overnight at 4 ˚C.   The following primary antibodies were used: anti-5mC mouse monoclonal antibody at 1:1000 (Calbiochem); anti-5hmC rabbit polyclonal antibody at 1:2000 (Active motif); anti-PCNA mouse monoclonal antibody at 1:1000 (Sigma); anti-BrdU rat monoclonal antibody at 1:200 (Abcam); anti-BrdU mouse monoclonal antibody at 1:100 (Amersham).   The following secondary antibodies were used: Alexa Fluor® 488 goat anti-rabbit IgG antibody at 1:500 (Invitrogen, Life Technologies Corp.); Alexa Fluor® 488 goat anti-rat IgG antibody at 1:500 (Invitrogen, Life Technologies Corp.); Alexa Fluor® 594 goat anti-mouse IgG antibody at 1:500 (Invitrogen, Life Technologies Corp.).   4',6-diamidino-2-phenylindole (DAPI) was used for nuclei staining at a concentration of 1:500.   For the negative control, we confirmed that no fluorescent signals are observed without a primary antibody or a secondary antibody (data not shown), and immunostaining pattern of 5mC or 5hmC is not changed when used a pre-absorbed primary antibody for 5mC or 5hmC (data not shown).

Image quantification

The images of immunohistochemical staining were captured using an Olympus FV1000-D confocal microscope with the same exposure times. The fluorescent signal intensities were measured in intra-ray nuclei within 500 mm from the amputation plane at 0 hpa, or in blastema nuclei at 24, 30, and 72 hpa by using the FluoView software. The 5mC or 5hmC signal intensity of individual nucleus in amputation site at 0 hpa or in blastema at 24, 30, and 72 hpa was normalized by their own DAPI signal intensity as an internal control. For non-amputated fins, the 5mC or 5hmC signal intensity was measured in intra-ray nuclei at the position of approximately two-third of fins, which is a common amputation site in this study, and they were normalized by their own DAPI signal intensity. At 0 hpa, the mean 5mC or 5hmC intensity of 600 randomly chosen intra-ray nuclei within 500 mm from the amputation plane in 6 different fish (approximately 100 nuclei per fish fin) is set as 1.0. Relative 5mC or 5hmC intensity of amputated fins at 24, 30, or 72 hpa is the normalized value by the mean 5mC or 5hmC intensity at 0 hpa, respectively. The 600 randomly chosen blastema nuclei from 6 different fish (approximately 100 nuclei per fish fin) were used for the calculation of relative 5mC or 5hmC intensity at 24, 30, or 72 hpa. And relative 5mC or 5hmC intensity of non-amputated fins is the normalized value by the mean 5mC or 5hmC intensity at 0 hpa, respectively. The 600 randomly chosen nuclei at the position of approximately two-third of non-amputated fins from 6 different fish (approximately 100 nuclei per fish fin) were used for the calculation of relative 5mC or 5hmC intensity. At 24 hpa, relative 5hmC intensity of individual blastema nucleus was classified as control or high level of 5hmC (Control/High level-5hmC) if they were greater than or equal to 0.98, and low level of 5hmC (Low level-5hmC) if they were less than 0.98 (5hmC intensity at 0 hpa: mean ± standard error, $1.0 ± 0.02$). *p*-values were calculated by using Student's *t* test.

BrdU incorporation assays

BrdU incorporation assays were performed as described previously [29]. Fin-amputated fish were allowed to regenerate in the fish water containing with 50 mg/ml BrdU until 24 hpa. After incubation, the regenerating fins were cut and BrdU-labeled cells were detected as described above.

Quantitative real-time PCR (qPCR)

For qPCR analyses, total RNA was extracted from the regenerating fins within 1000 mm from the amputation plane at 0 hpa (3 regenerates per extraction), 18 hpa (5 regenerates per extraction), and 30 hpa (5 regenerates per extraction), and from the blastema at 72 hpa (3 regenerates per extraction) using TRIzol (Invitrogen, Life Technologies Corp.).   Reverse transcription (RT)-negative control was performed to test for the genomic DNA contamination using RT-PCR and no amplification was found in any samples (data not shown).   Three hundred nanograms of DNase-treated RNA was reverse transcribed using oligo-(dT) primers and Reverse transcriptase XL (Takara).   qPCR for nine genes (*gadd45ba*, *gadd45bb*, *gadd45g*, *apobec2b*, *tdg*, *mbd4*, *tet2*, *tet3*, and *parp1*) was performed in tetraplicates using the Thermal Cycler Dice® Real Time System, SYBR® *Premix Ex Taq™* (TaKaRa Bio Inc.) according to the manufacturer's instructions.   Because both zebrafish *actb1* and *ribosomal protein L13a* (*rpl13a*) were stably expressed in fins or fin regenerates (data not shown), *actb1* was used as reference gene for qPCR.   All primer pairs were designed to span an intron-exon boundary to prevent amplification of genomic DNA and the amplified signals were confirmed to be a single band by gel electrophoresis.   No template control was performed for nine genes to confirm the specificity of qPCR (data not shown).   Detailed qPCR conditions used to amplify each of nine genes are listed in Supplementary Table.   *p*-values were calculated by using Student's *t* test.

Acknowledgements

# References

1. Wu SC, Zhang Y. Active DNA demethylation: many roads lead to Rome. Nat Rev Mol Cell Biol 2010; 11:607-20.

2. Cedar H, Bergman Y. Programming of DNA methylation patterns. Annu Rev Biochem 2012; 81:97-117.

3. Franchini DM, Schmitz KM, Petersen-Mahrt SK. 5-Methylcytosine DNA Demethylation: More Than Losing a Methyl Group. Annu Rev Genet 2012.

4. Goll MG, Bestor TH. Eukaryotic cytosine methyltransferases. Annu Rev Biochem 2005; 74:481-514.

5. Jones PA. Functions of DNA methylation: islands, start sites, gene bodies and beyond. Nat Rev Genet 2012; 13:484-92.

6. Zhu JK. Active DNA demethylation mediated by DNA glycosylases. Annu Rev Genet 2009; 43:143-66.

7. Niehrs C, Schäfer A. Active DNA demethylation by Gadd45 and DNA repair. Trends Cell Biol 2012; 22:220-227.

8. Branco MR, Ficz G, Reik W. Uncovering the role of 5-hydroxymethylcytosine in the epigenome. Nat Rev Genet 2012; 13:7-13.

9. Williams K, Christensen J, Helin K. DNA methylation: TET proteins-guardians of CpG islands? EMBO Rep 2012; 13:28-35.

10. Tan L, Shi YG. Tet family proteins and 5-hydroxymethylcytosine in development and disease. Development 2012; 139:1895-1902.

11. Akimenko MA, Marí-Beffa M, Becerra J, Géraudie J. Old questions, new tools, and some answers to the mystery of fin regeneration. Dev Dyn 2003; 226:190-201.

12. Poss KD, Keating MT, Nechiporuk A. Tales of regeneration in zebrafish. Dev Dyn 2003; 226:202-210.

13. Tanaka EM, Reddien PW. The cellular basis for animal regeneration. Dev Cell 2011; 21:172-185.

14. Slack JM. Amphibian muscle regeneration--dedifferentiation or satellite cells? Trends Cell Biol 2006; 16:273-275.

15. Barrero MJ, Izpisua Belmonte JC. Regenerating the epigenome. EMBO Rep 2011; 12:208-215.

16. Katsuyama T, Paro R. Epigenetic reprogramming during tissue regeneration. FEBS Lett 2011; 585:1617-1624.

17. Thummel R, Burket CT, Hyde DR. Two different transgenes to study gene silencing and re-expression during zebrafish caudal fin and retinal regeneration. ScientificWorldJournal 2006; 6 Suppl 1:65-81.

18. Yakushiji N, Suzuki M, Satoh A, Sagai T, Shiroishi T, Kobayashi H, et al. Correlation between Shh expression and DNA methylation status of the limb-specific Shh enhancer region during limb regeneration in amphibians. Dev Biol 2007; 312:171-182.

19. Martin CC, Laforest L, Akimenko MA, Ekker M. A role for DNA methylation in gastrulation and somite patterning. Dev Biol 1999; 206:189-205.

20. Mhanni AA, McGowan RA. Global changes in genomic methylation levels during early development of the zebrafish embryo. Dev Genes Evol 2004; 214:412-417.

21. MacKay AB, Mhanni AA, McGowan RA, Krone PH. Immunological detection of changes in genomic DNA methylation during early zebrafish development. Genome 2007; 50:778-785.

22. Almeida RD, Loose M, Sottile V, Matsa E, Denning C, Young L, et al. 5-hydroxymethyl-cytosine enrichment of non-committed cells is not a universal feature of vertebrate development. Epigenetics 2012; 7:383-389.

23. Urasaki A, Morvan G, Kawakami K. Functional dissection of the Tol2 transposable element identified the minimal cis-sequence and a highly repetitive sequence in the subterminal region essential for transposition. Genetics 2006; 174:639-649.

24. Woods AL, Hall PA, Shepherd NA, Hanby AM, Waseem NH, Lane DP, et al. The assessment of proliferating cell nuclear antigen (PCNA) immunostaining in primary gastrointestinal lymphomas and its relationship to histological grade, S+G2+M phase fraction (flow cytometric analysis) and prognosis. Histopathology 1991; 19:21-27.

25. Powell C, Elsaeidi F, Goldman D. Injury-dependent Müller glia and ganglion cell reprogramming during tissue regeneration requires Apobec2a and Apobec2b. J Neurosci 2012; 32:1096-109.

26. Poleo G, Brown CW, Laforest L, Akimenko MA. Cell proliferation and movement during early fin regeneration in zebrafish. Dev Dyn 2001; 221:380-390.

27. Tittle RK, Sze R, Ng A, Nuckels RJ, Swartz ME, Anderson RM, et al. Uhrf1 and Dnmt1 are required for development and maintenance of the zebrafish lens. Dev Biol 2011; 350:50-63.

28. MacKay AB, Mhanni AA, McGowan RA, Krone PH. Immunological detection of changes in genomic DNA methylation during early zebrafish development. Genome 2007; 50:778-785.

29. Nechiporuk A, Keating MT. A proliferation gradient between proximal and msxb-expressing distal blastema directs zebrafish fin regeneration. Development 2002; 129:2607-17.

Figures
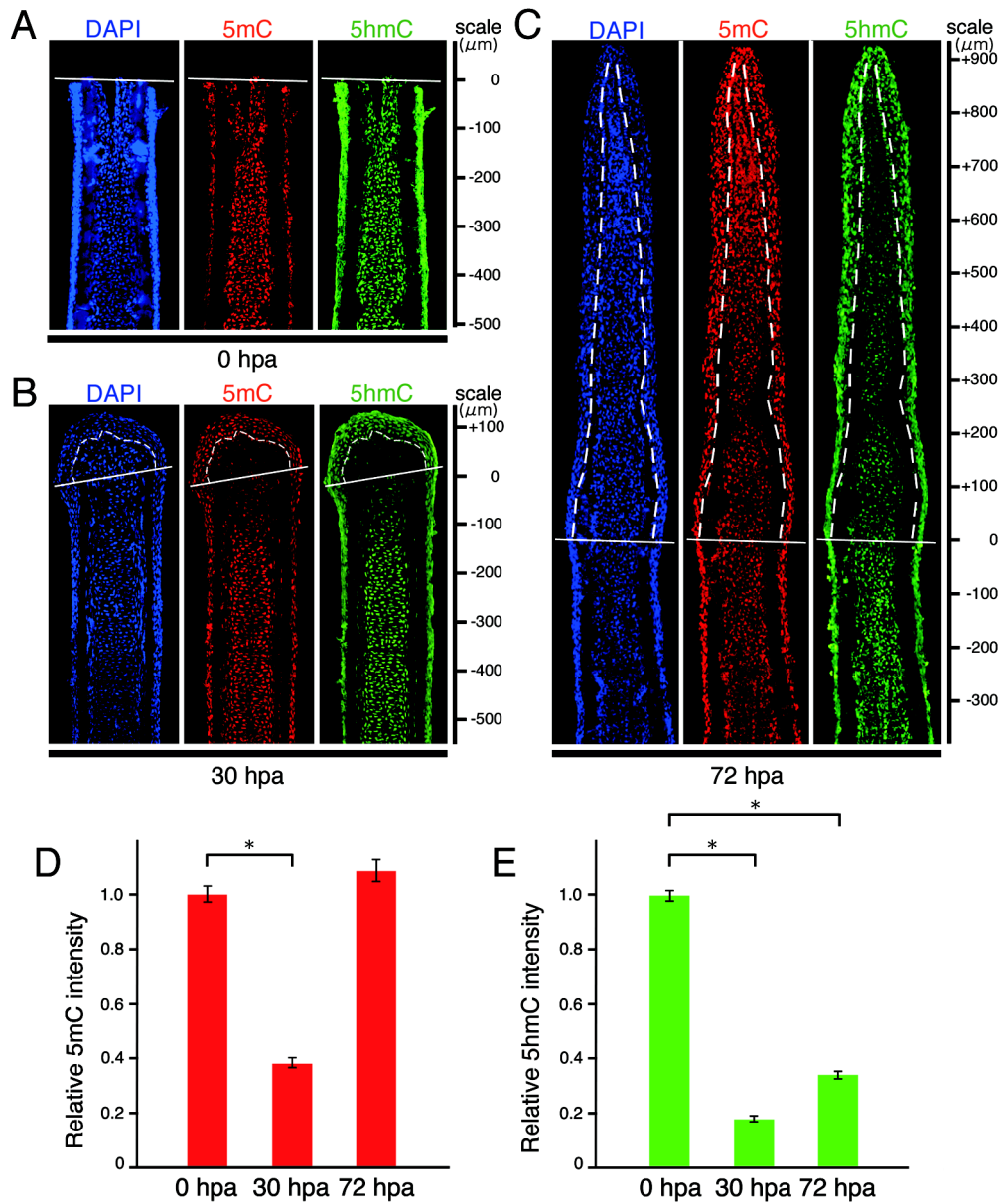
Fig. 1. Spatial and temporal distributions of 5mC and 5hmC during regeneration of zebrafish fin

(A-C) Longitudinal sections of wild-type fin regenerates that were immunohistochmically stained with antibodies against 5mC (red) and 5hmC (green) at 0 (A), 30 (B), and 72 hpa (C).   The fluorescent signals of DAPI (blue) indicate the presence of nuclei.   Uniform distributions of 5mC and 5hmC fluorescent signals were observed in the intra-ray cells at 0 hpa (A).   The fluorescent signals of both 5mC and 5hmC in the balstema cells and cells within 150 mm proximal to the amputation plane at 30 hpa were lower than those at 0 hpa (B).   At 72 hpa, the 5mC level in the blastema

cells was almost restored, whereas the 5hmC level in the blastema cells was still lower than that at 0 hpa (C).   White lines indicate the amputation planes.   Dashed lines outline the basement membrane, which shows the boundary between the epidermis and blastema.   Scale bars represent the distance from the amputation plane.   (D, E) Quantification of the relative fluorescent signal of 5mC or 5hmC at 0, 30, and 72 hpa. Relative 5mC intensity at 30 hpa and relative 5hmC intensities at 30 and 72 hpa were significantly lower than those at 0 hpa.   In contrast, relative 5mC intensity at 72 hpa was almost same as that at 0 hpa.   * $p < 0.001$ by Student's t- test.   Error bars represent the standard error.
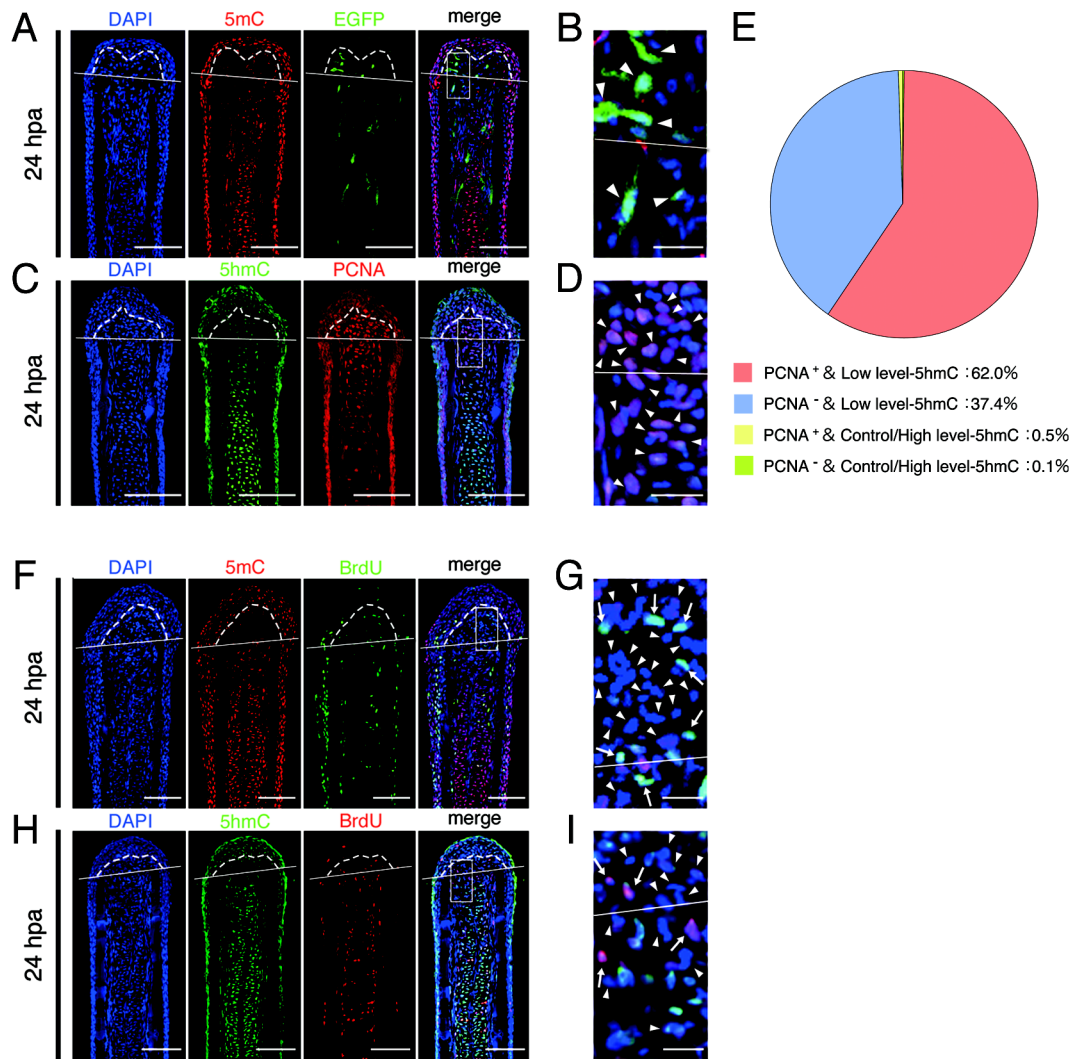
Fig. 2. Down-regulation of 5mC or 5hmC level is associated with active demethylation

(A, B) Longitudinal sections of Tg(*ef1-a:EGFP*) fin regenerates that immunohistochemimally stained with an antibody against 5mC at 24 hpa. Merged images revealed that some cells, which show low level of 5mC, are EGFP fluorescence positive in the blastema cells and cells adjacent to amputation plane (A, arrowheads in B). The boxed area in A is shown enlarged in B. (C-E) Longitudinal sections of wild-type fin regenerates that were co-stained with antibodies against 5hmC and PCNA at 24 hpa (C). The boxed area in C is shown enlarged in D. Quantification of the relative 5hmC intensity and PCNA in the blastema area at 24 hpa (E). Merged images and quantification data revealed that majority of the blastema nuclei (62.0%) shows PCNA positive and low level of 5hmC (E, C, arrowheads in D). Control/High

level-5hmC: control or high level of 5hmC, Low level-5hmC: low level of 5hmC. (F-I) Longitudinal sections of wild-type fin regenerates that were co-stained with antibodies against 5mC/5hmC and BrdU at 24 hpa, respectively.   BrdU is not incorporated in almost all blastema cells and cells adjacent to amputation plane that show lower level of 5mC or 5hmC (E, G, arrowheads in F and H).   However, BrdU is incorporated in some blastema cells and cells adjacent to the amputation plane, which show lower level of 5mC or 5hmC (arrows in F and H).   The boxed areas in E and G are shown enlarged in F and H, respectively.   White lines indicate the amputation planes.   Dashed lines outline the basement membrane, which shows the boundary between the epidermis and blastema.   Scale bars:100 mm in A, C, E, and G; 20 mm in B, D, F, and H.
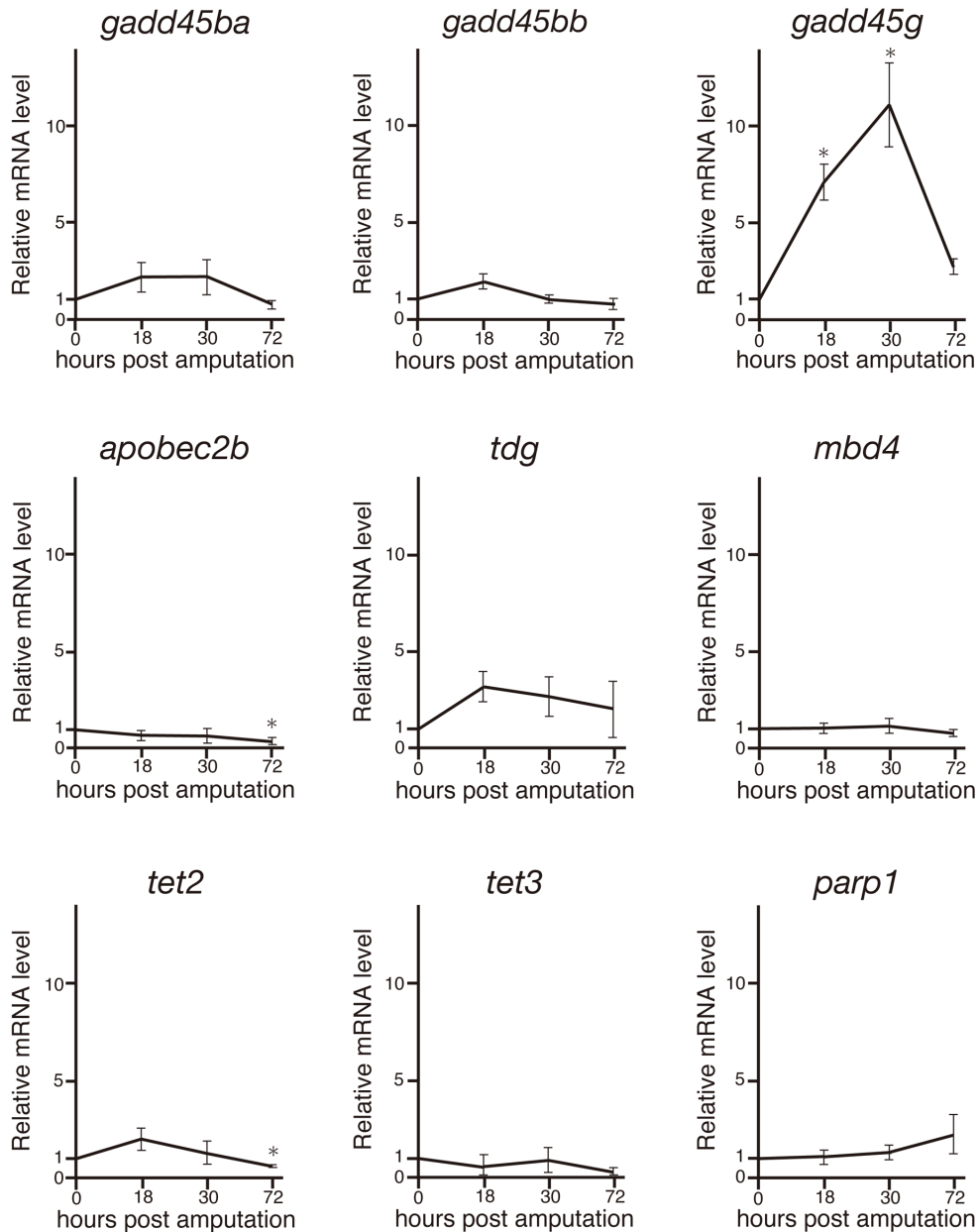
Fig. 3. Relative expressions of demethylation- and DNA repair-related genes during regeneration of zebrafish fin by qPCR

Expressions of demethylation- and DNA repair-related genes were examined via qPCR at 0, 18, 30, and 72 hpa. The expression level at 0 hpa is set as 1.0, and the relative mRNA levels (y-axis) at 18, 30, and 72 hpa of each gene were shown. The relative expressions of *gadd45ba, gadd45bb, apobec2b, tdg, mbd4, tet2, tet3,* and *parp1* were

not markedly up-regulated after regeneration. In contrast, the relative expression of *gadd45g* was significantly up-regulated at 18 and 30 hpa. $* p < 0.001$ by Student's *t*-test. Error bars represent the standard error of three independent experiments.
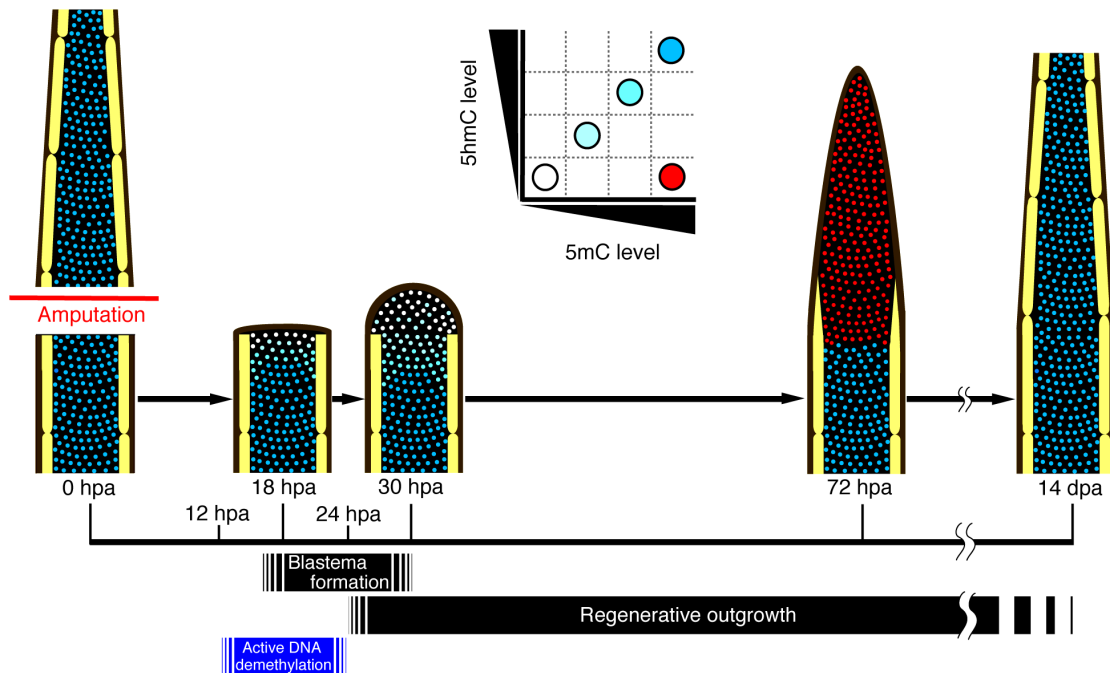
Fig. 4. Spatial and temporal changes of 5mC and 5hmC levels during regeneration of zebrafish fin

A proposed model for 5mC or 5hmC level during regeneration of zebrafish fin based on our findings. Schematic representations of a longitudinal section of a fin ray. The level of 5mC or 5hmC in the cells adjacent to the amputation plane starts to reduce from approximately at 12 hpa, and the number of demethylated cells increases until 24 hpa by active demethylation. Subsequently, these demethylated cells start to proliferate, so that the number of blastema cells is increased. By 72 hpa, the 5mC level is up-regulated, probably because DNA remethylation occurs in the blastema cells. In contrast to that of 5mC, the 5hmC level is still reduced in the blastema cells at 72 hpa and is gradually recovered by 14 dpa.

36

Supplemental figures
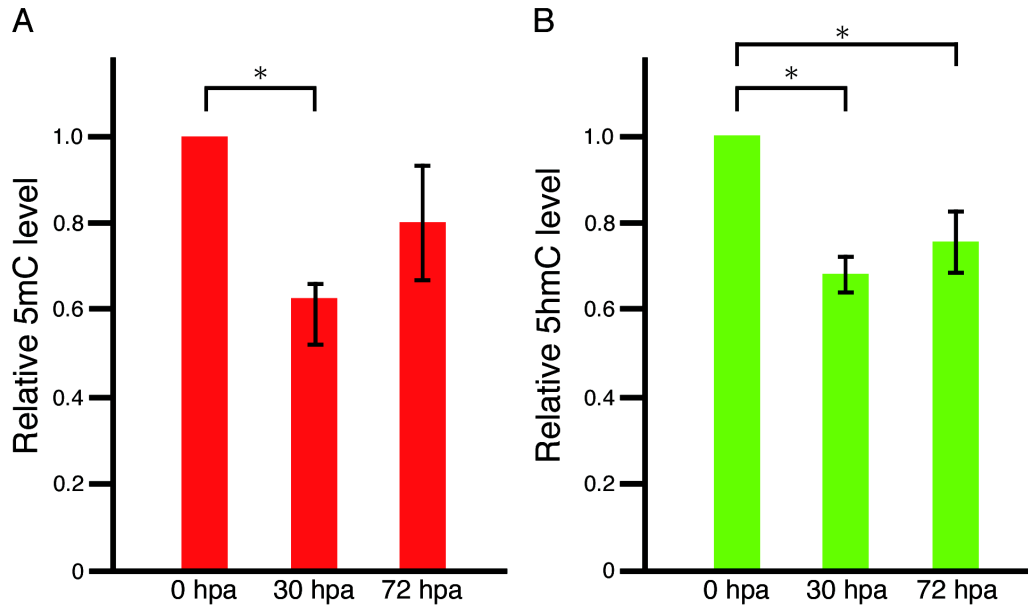
Fig. S1. Quantification of 5mC and 5hmC levels during regeneration of zebrafish fin

(A, B) Relative levels of 5mC and 5hmC at 30 and 72 hpa compared with those at 0 hpa. Average signal intensity for 5mC or 5hmC at 0 hpa is set as 1.0. * $p < 0.001$ by Student's *t*-test. Error bars represent the standard error.
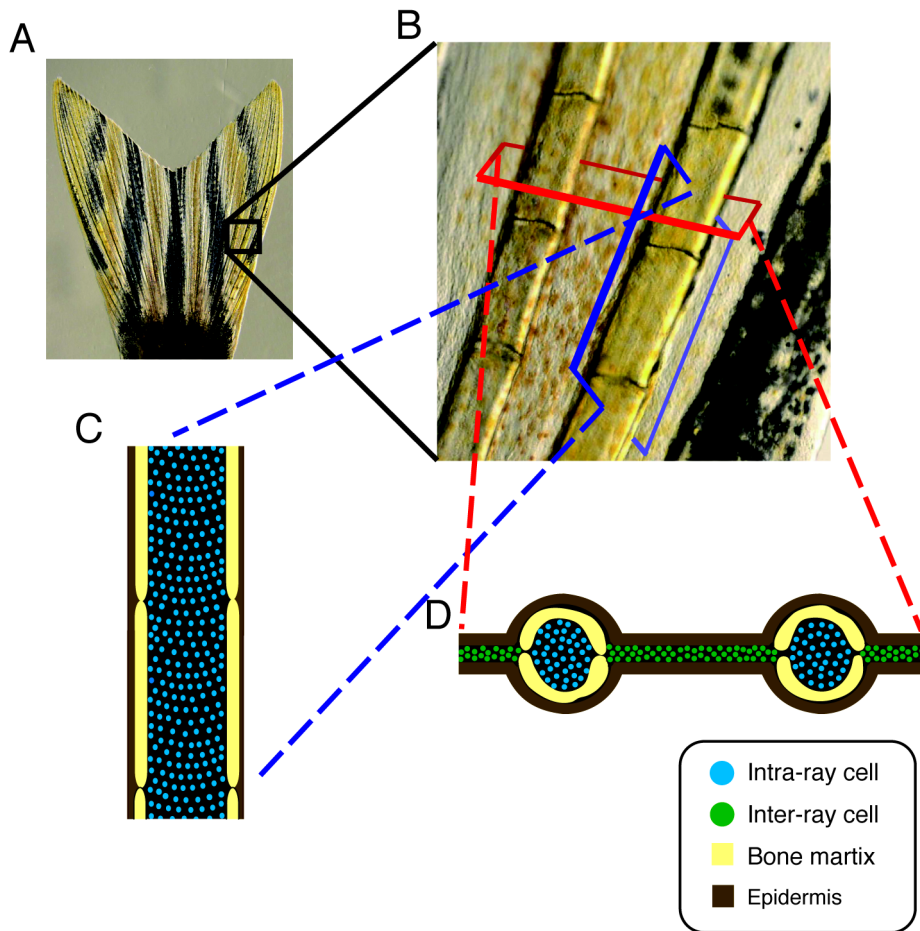
Fig. S2. Structure of adult zebrafish caudal fin

(A, B) A picture of adult zebrafish caudal fin (A) and an enlarged image of fin rays (B).   (C) Longitudinal section of a fin ray.   (D) Cross section of 2 fin rays.
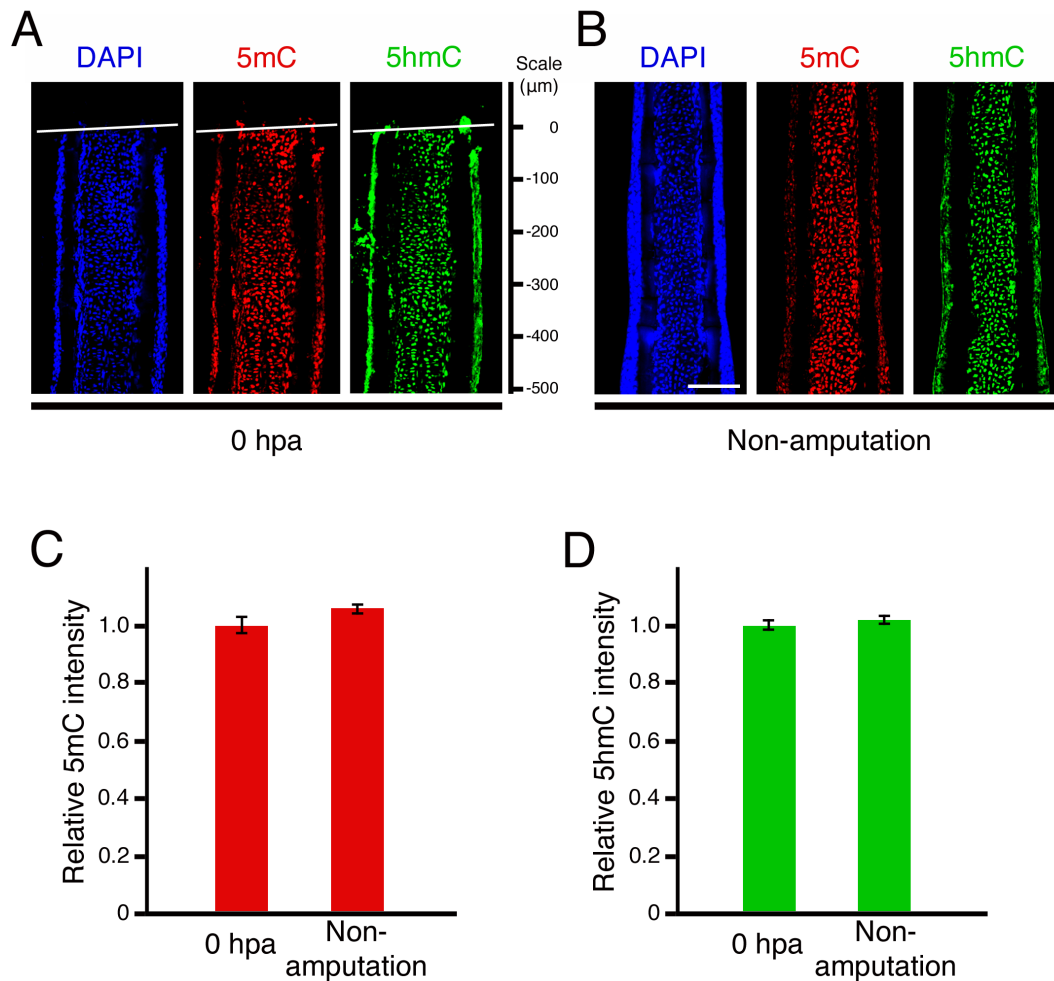
Fig. S3. Relative 5mC or 5hmC level was not changed between in fins at 0 hpa and in the non-amputated fins

(A, B) Longitudinal sections of a fin at 0 hpa (A) and an non-amputated fin (B) that were immunohistochmically stained with antibodies against 5mC (red) and 5hmC (green). The fluorescent signals of DAPI (blue) indicate the presence of nuclei. The intensity of DAPI, 5mC, or 5hmC was shown at the position of approximately two-third of fins, which is a common amputation site in this study (B). (C, D) Relative 5mC or 5hmC was not changed between in fins at 0 hpa and in the non-amputated fins. White lines indicate the amputation planes. Scale bars represent 100 mm. * $p < 0.001$ by Student's t- test. Error bars represent the standard error.
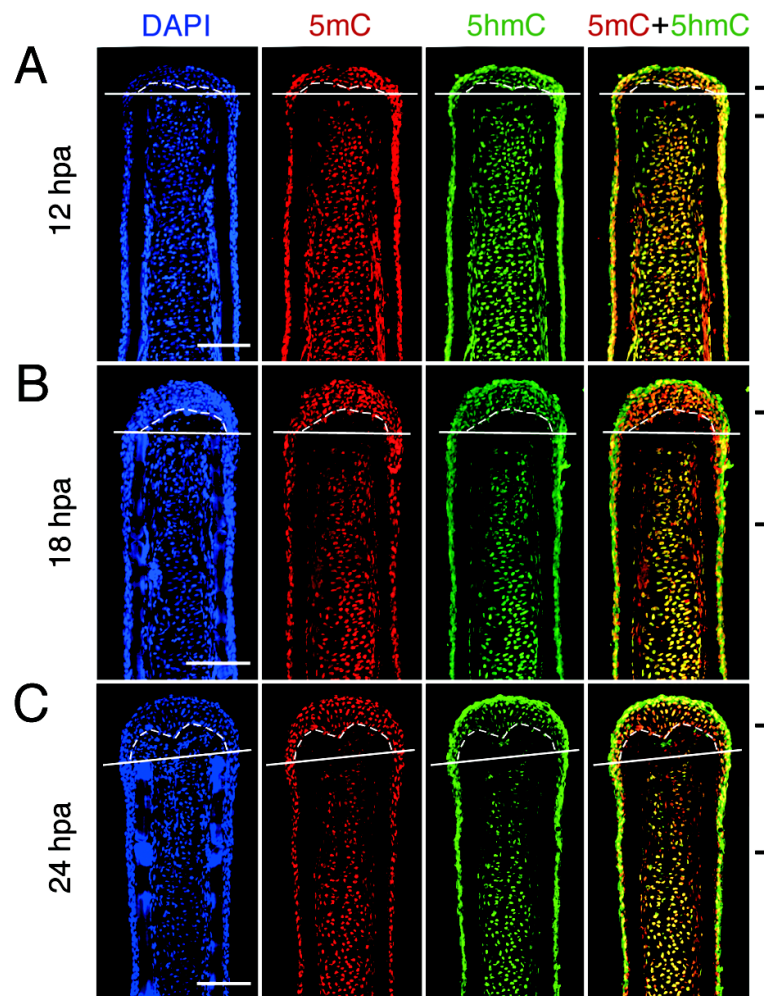
Fig. S4. Reduction of 5mC and 5hmC levels during regeneration of zebrafish fin

(A-C) Longitudinal sections of wild-type fin regenerates that were immunohistochmically stained with antibodies against 5mC (red) and 5hmC (green) at 12 (A), 18 (B), and 24 hpa (C). Blastema cells and cells adjacent to the amputation plane showed reduced levels of 5mC and 5hmC (brackets in A, B, C). The fluorescent signals of DAPI (blue) indicate the presence of nuclei. White lines indicate the amputation planes. Dashed lines outline the basement membrane, which shows the boundary between the epidermis and blastema. Scale bars represent 100 mm.
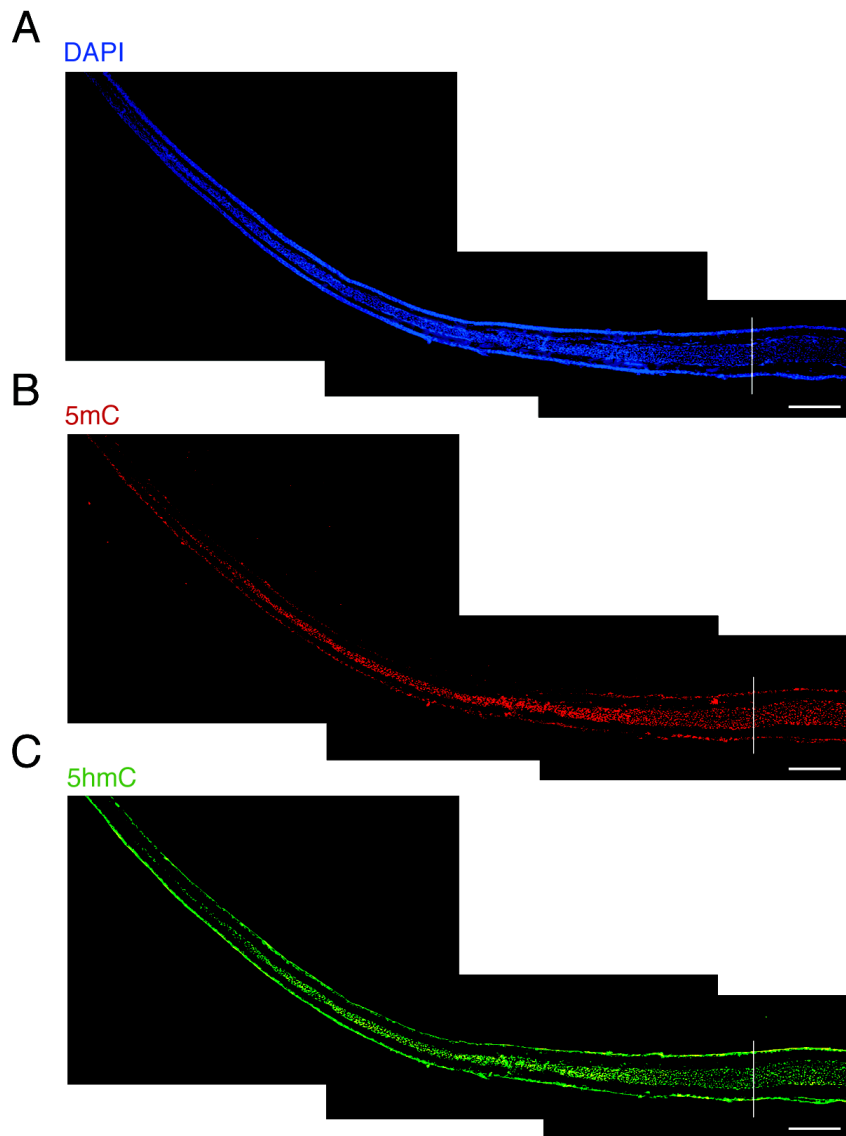
Fig. S5. Distributions of 5mC and 5hmC at 14 dpa

(A-C) Longitudinal sections of wild-type fin regenerates that were immunohistochmically stained with antibodies against 5mC (B) and 5hmC (C) at 14 dpa.   The fluorescent signals of DAPI (A) indicate the presence of nuclei.   White lines indicate the putative amputation planes. Scale bars represent 200 mm.
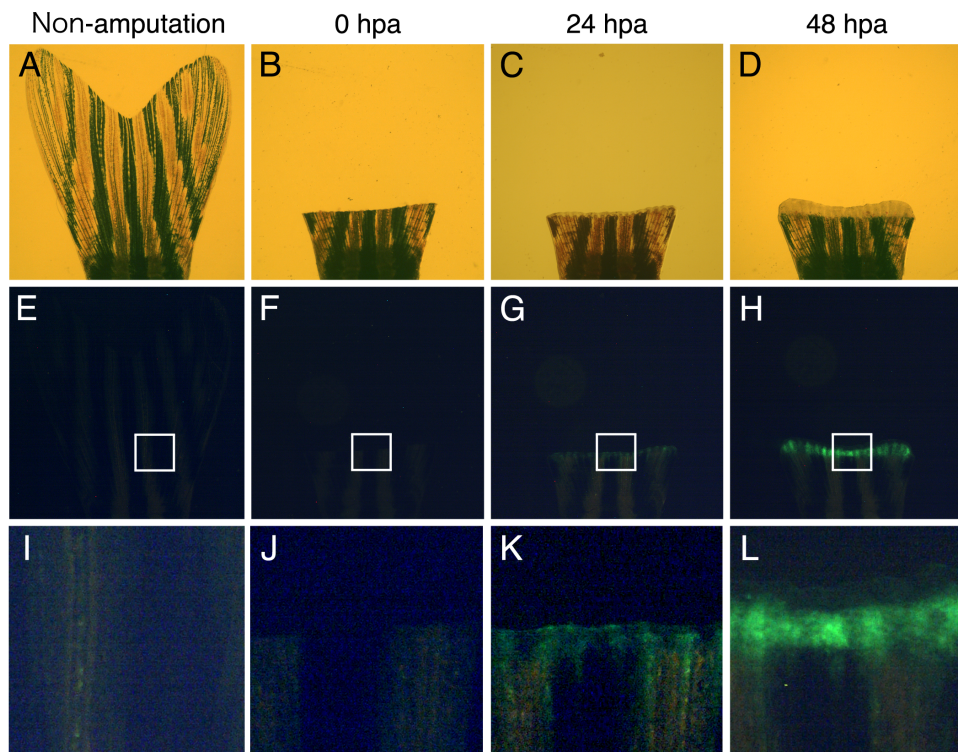
Fig. S6. EGFP fluorescence of Tg(*ef1-a:EGFP*) transgenic fish was not detected before amputation and at 0 hpa.

(A-D) Bright field images of Tg(*ef1-a:EGFP*) transgenic fish fins before and after amputation.   (E-L) Fluorescence images of Tg(*ef1-a:EGFP*) transgenic fish fins before and after amputation.   The boxed areas in E, F, G, and H are shown enlarged in I, J, K, and L, respectively.   No EGFP fluorescence was detected before amputation and at 0 hpa (E, F, I, J).   Scale bars represent 100 mm.

Supplementary Table : Primer sequences and PCR conditions

Gene	Sequence		Ref.	Annealing temperature
gadd45ba	forward: TCTCACAGTCGGCGTTTATG		1	56°C
	reverse: CGGCTCTCCTCACAGTAGGT			
gadd45bb	forward: GATCCACTTCACGCTCATCCA		2	56°C
	reverse: GGCAATAGAAGGCACCCACTG			
gadd45g	forward: CAACGACATCAACATCGTTCG		1	56°C
	reverse: TCAGCGTTCAGGCAGAGTAA			
apobec2b	forward: ACATACAAGGTGGAGCAGCAGAG			60°C
	reverse: AAATCCACAGGCCTCATCATGCG			
tdg	forward: ATGGATGAAAGGCTGTATGGATC		1	60°C
	reverse: TCCTCTGGATGTACAGGCAT			
mbd4	forward: CTTCTGCTCAGCGTTCACAACTC			60°C
	reverse: CATGGCTCTGTGCAGATCTTCAC			
tet2	forward: CACACCCAACTCTAAAACGGACAACAC		2	60°C
	reverse: ATGGTGGGGAAGCGTAAGAAGGA			
tet3	forward: GGACTGTCGTCTGGGCTGTAGGG		2	62°C
	reverse: GCCAGCAGCCGCACTTCTCTT			
parp1	forward: ATCAGACGTCTCTGTGGTGAGAC			60°C
	reverse: CTTGCAGCAGGCTATATCCTAGC			
actb1	forward: CCGTGACATCAAGGAGAAGCT			60°C
	reverse: TCATGGATACCGCAAGATTCC			
rpl13a	forward: TCTGGAGGACTGTAAGAGGTATGC		3	56°C
	reverse: AGACGCACAATCTTGAGAGCAG			
apobec2a	forward: TCAAGAACGTGGAGTACTCGTCC			58°C
	reverse: TTCCAAGTGTGTGCGTCGACTAG			
aid	forward: GACGGTGCAAGATTGTGTTAC			56°C
	reverse: TAAGTCATGACCGAGATCTGAAC			

References
1. Rai K, Huggins IJ, James SR, Karpf AR, Jones DA, Cairns BR. DNA demethylation in zebrafish involves the coupling of a deaminase, a glycosylase, and gadd45.
Cell 2008; 135:1201-12.
2. Powell C, Elsaeidi F, Goldman D. Injury-dependent Müller glia and ganglion cell reprogramming during tissue regeneration requires Apobec2a and Apobec2b.
J Neurosci 2012; 32:1096-109.
3. Tang R, Dodd A, Lai D, McNabb WC, Love DR. Validation of zebrafish (Danio rerio) reference genes for quantitative real-time RT-PCR normalization.
Acta Biochim Biophys Sin (Shanghai) 2007; 39:384-90.

Chapter 3. Mechanistic target of rapamycin complex 1 signaling regulates cell proliferation, cell survival, and differentiation in regenerating zebrafish fins

Abstract

The mechanistic target of rapamycin complex1 (mTORC1) signaling pathway has been implicated in functions of multicellular processes, including cell growth and metabolism, although mTORC1 function remains unknown. To investigate the role of mTORC1 signaling pathway in zebrafish caudal fin, we examined the activation and function of mTORC1 signaling using an antibody against phosphorylated S6 kinase and a specific inhibitor, rapamycin. mTORC1 signaling is activated in proliferative cells of intra-ray and wound epidermal cells before blastema formation, as well as in proliferative blastema cells, wound epidermal cells, and osteoblasts during regenerative outgrowth. Before blastema formation, proliferation of intra-ray and wound epidermal cells is suppressed, but cell death is not affected by mTORC1 signaling inhibition with rapamycin. Moreover, rapamycin treatment inhibits blastema and wound epidermal cell proliferation and survival during blastema formation and regenerative outgrowth, as well as osteoblast proliferation and differentiation during regenerative outgrowth. We further determined that mTORC1 signaling is regulated through IGF-1 receptor/phosphatidylinositol-3 kinase and Wnt pathways during fin regeneration. Taken together, our findings reveal that mTORC1 signaling regulates proliferation, survival, and differentiation of intra-ray cells, wound epidermis, blastema cells, and/or osteoblasts in various fin regeneration stages downstream of IGF and Wnt signaling pathways.

Introduction

Mammalians present a limited ability for organ regeneration, whereas various non-mammalian vertebrates such as teleosts and urodele amphibians show outstanding regeneration ability. Among them, the zebrafish is a useful animal model, which has been used to study the regeneration of several organs or appendages [1,2]. The adult zebrafish caudal fin is composed of multiple cell types, including fibroblast-like mesenchymal cells, osteoblasts, endothelial cells, neurons, and epidermal cells, and the fin regeneration process presents three stages: pre-blastema formation, blastema formation, and regenerative outgrowth [3,4,5]. Following fin amputation, epidermal cells migrate to cover the wound within 12 hours post amputation (hpa) [5]. The intra-ray mesenchymal cells and osteoblasts then migrate toward the amputation plane by 24 hpa (pre-blastema formation stage) [5]. From 18 to 24 hpa, these intra-ray mesenchymal cells and osteoblasts begin to proliferate [3] and, as a result, a population of these cells, named blastema, is formed underneath the wound epidermis by 48 hpa (blastema formation stage). After 48 hpa, regenerative outgrowth starts and the ray blastema mainly consists of three distinct domains: the distal blastema, proliferative zone, and differentiation zone (72 hpa, Figure 2P) [5,6]. The distal blastema barely contains proliferative blastema cells, and the proliferative zone contains highly proliferative mesenchymal cells (the proximal medial blastema) and osteoblasts (72 hpa, Figure 2P) [3,5,6].

Since rapamycin presents various physiological functions such as antifungal, immunosuppressive, and antiproliferative properties, many researchers have focused on the identification of rapamycin intracellular targets [7]. Mechanistic target of rapamycin (mTOR), a serine/threonine kinase, has been shown to be a rapamycin target in yeast, and most eukaryotes have this protein [7,8]. The mTOR signaling pathway is mainly involved in cell growth and metabolism as two distinct complex types, mTOR complex 1 (mTORC1) and 2 (mTORC2) [7,8]. The mTORC1 signaling pathway is involved in multicellular processes, including protein synthesis, lipid synthesis, glycolysis, and autophagy, and is specifically inhibited by rapamycin [7,8]. mTORC1 signaling is known to regulate protein synthesis mainly through direct phosphorylation of S6 kinase (S6K) [7,8].

Many signaling pathways, including Activin, Bmp, Fgf, sonic hedgehog,

Insulin-like growth factor (IGF), Notch, retinoic acid, Wnt, and reactive oxygen species (ROS), are implicated in the regulation of cell proliferation and/or differentiation in non-mammalian vertebrate regeneration, also known as epimorphic regeneration [2,9,10,11,12]. However, the spatiotemporal activation and function of the mTORC1 signaling pathway during epimorphic regeneration remains unknown. In this study, we explored the activation and function of mTORC1 signaling during various stages of zebrafish caudal fin regeneration, and identified the upstream signaling pathway leading to mTORC1 signaling activation during caudal fin regeneration.

Results

Spatiotemporal dynamism of mTORC1 signaling activation during fin regeneration

To investigate the molecular mechanisms of regeneration, we analyzed the signaling pathways involved in zebrafish fin regeneration using various inhibitors and drugs. Our experiments indicated that rapamycin, a well-known inhibitor of mTORC1 signaling, presented a strong inhibitory effect on fin regeneration. To analyze the activation of mTORC1 signaling during fin regeneration, spatiotemporal distribution of phosphorylated S6 kinase (p-S6K), an activated form of S6K, was first examined by immunohistochemistry. Although no p-S6K-positive cells were found in intra-ray and epidermal cells immediately after fin amputation (0 hpa) (Figure 1A), p-S6K signals were detected as early as 6 hpa (Figure 1B). The number of p-S6K-positive cells in the intra-ray, epidermis, and blastema was markedly increased, and p-S6K-positive cell localization gradually changed with the progression of fin regeneration. These p-S6K-positive cells were widely distributed in the intra-ray and wound epidermis proximal to the amputation plane from 6 to 18 hpa (arrowheads in Figure 1B-D). From 24 hpa, these cells started to accumulate underneath the wound epidermis, and p-S6K-positive blastema cells were evident at 36 hpa (arrowheads in Figure 1E,F). After 48 hpa, p-S6K-positive cells were mainly detected in the blastema and wound epidermis. At 72 and 120 hpa, p-S6K signals were restricted to three distinct domains in the blastema, the putative proximal medial blastema domain (arrowheads in Figure 1H,I') [3], the bilateral stripped-domains (arrows in Figure 1H,I'), where differentiating osteoblasts and their progenitor cells are localized [11,13], and the wound epidermis. On the other hand, it is interesting to note that p-S6K signals were absent in the tip of the putative proximal medial blastema domain and putative distal blastema (brackets in Figure 1G,H,I'). These results suggest that, although the mTORC1 signaling pathway is widely activated in the intra-ray, wound epidermal cells, and blastema cells until 48 hpa, mTORC1 signaling is gradually restricted to the putative proliferative blastema cells and osteoblasts after 72 hpa.

To characterize p-S6K-positive cells during the pre-blastema formation (24 hpa) and regenerative outgrowth stages (72 hpa), the fin regenerates were co-immunostained with proliferating cell nuclear antigen (PCNA), a marker for proliferative cells [14];

Zns-5, a marker for all osteoblasts independent of differentiation stages [15]; or Runx2, an osteoblast progenitor marker [16]. At 24 hpa, almost all p-S6K-positive intra-ray and blastema cells were PCNA-positive (Figure 2A-C'), and all Runx2-positive osteoblast progenitors were p-S6K-positive (Figure 2D-F'), suggesting that mTORC1 signaling is active in proliferative cells and osteoblast progenitors during the pre-blastema formation stage. At 72 hpa, PCNA-positive cells in the putative proximal medial blastema domain were p-S6K-positive (arrowheads in Figure 2I'), except that the tip of the putative proximal medial blastema domain (a bracket in Figure 2I') was p-S6K-negative. In the bilateral-stripped domains, Zns-5- or Runx2-positive cells were p-S6K-positive (arrowheads in Figure 2L',O'), except in the most distal regions of these domains (brackets in Figure 2L',O'). A recent report showed that Runx2-positive self-renewing preosteoblasts are localized in the most distal region and that Runx2/Sp7 (Osterix) double-positive cells are differentiating osteoblasts [11]. Our results suggest that mTORC1 signaling is active in proliferative blastema cells and differentiating osteoblasts during the regenerative outgrowth stage. These spatiotemporal mTORC1 activation patterns prompted us to further analyze the function of mTORC1 signaling in the pre-blastema formation, blastema formation, and regenerative outgrowth stages.

mTORC1 signaling is required for cell proliferation, but not for cell survival during the pre-blastema formation stage

To examine the function of mTORC1 signaling during fin regeneration, adult zebrafish were treated with a specific mTORC1 inhibitor, rapamycin, 12 h before amputation (-12 h) to 72 hpa (Figure 3A). Rapamycin significantly inhibited fin regeneration compared to DMSO (Figure 3B,C). In addition to rapamycin, we examined the two different pharmacological inhibitors, Torin1 [17] and AZD8055 [18], in mTOR signaling inhibition, and found that fin regeneration was also significantly inhibited by both Torin1 and AZD8055 treatment (Figure S1). mTORC1 signaling inhibition, by rapamycin, Torin1, and AZD8055 was confirmed by the loss of p-S6K signal at 72 hpa (Figure S2). The p-S6K signals were markedly reduced by 3 h treatment with these inhibitors (rapamycin, Torin1, and AZD8055) and were nearly diminished by 6 h treatment (Figure S3), suggesting the specificity of p-S6K as readout of mTORC1 signaling. Furthermore, fin regeneration was also inhibited by the

knockdown of *raptor*, which encodes a component of mTORC1 [7,8,19] using a morpholino antisense oligo nucleotide (MO) (Figure S4).   Taken together, inhibition of mTORC1 signaling with these three inhibitors (rapamycin, Torin1, and AZD8055) or by knockdown of *raptor* suggests that mTORC1 signaling is required in the pre-blastema formation, blastema formation, and regenerative outgrowth stages during fin regeneration.

We showed that mTORC1 signaling is active in proliferative intra-ray cells and osteoblast progenitors during the pre-blastema formation stage (Figure 2A-F').   To test whether mTORC1 signaling affects cell proliferation before blastema formation, PCNA and Runx2 immunohistochemical staining, a BrdU incorporation assay, and expression of *msxb* [20] and the *Xenopus ef1-a:EGFP* transgene using the transgenic fish XIG8A [Tg(*ef1- a;EGFP*)] [21] were performed in rapamycin-treated fins.   Because cell proliferation starts at approximately 18 hpa in regenerating fins [3], inhibition experiments of mTORC1 signaling by rapamycin treatment were performed from -12 h to 18 hpa (or 24 hpa).   mTORC1 signaling inhibition was confirmed by the loss of the p-S6K signal at 24 hpa (Figure S5).   At 18 hpa, the number of PCNA-positive cells and the percent of Runx2-positive cells were significantly reduced by rapamycin treatment (Figure 4B-E), whereas the number of apoptotic cells was not increased in the intra-ray and epidermal cells (Figure 4F,G), indicating that inhibition of mTORC1 signaling suppresses cell proliferation without inducing apoptosis.   Consistent with PCNA and Runx2 immunohistochemical staining, the number of BrdU incorporated cells in both the intra-ray and epidermis was significantly reduced by the rapamycin treatment at 24 hpa (Figure 4H,I).   It was previously reported that *msxb* and *Xenopus ef1-a:EGFP* transgene are molecular markers for mesenchymal progenitor cells [20] and proliferative cells [22] in the regenerating fins, respectively.   Similarly to PCNA and Runx2 expression, *msxb* and *Xenopus ef1-a:EGFP* transgene expression was markedly decreased by rapamycin treatment at 24 hpa as determined by whole-mount *in situ* hybridization and EGFP fluorescence, respectively (Figure 4J,K).   These results clearly indicate that mTORC1 signaling is required for cell proliferation, but not in cell survival of intra-ray and epidermal cells before blastema formation.

mTORC1 signaling is required for cell proliferation and cell survival during the regenerative outgrowth stage

Because p-S6K-positive cells start to accumulate underneath the wound epidermis from 24 hpa (Figure 1E), and cell proliferation is suppressed until 24 hpa by mTORC1 signaling inhibition (Figure 4), identifying the function of mTORC1 signaling during blastema formation and regenerative outgrowth is difficult.   We next examined the function of mTORC1 signaling during the blastema formation and regenerative outgrowth stages using rapamycin from 24 to 72 hpa (Figure 5A).   Regenerative outgrowth was significantly inhibited by rapamycin treatment from 24 to 72 hpa (Figure 5B,C), as observed by rapamycin treatment from -12 h to 72 hpa (Figure 3).   mTORC1 signaling inhibition was confirmed by the loss of the p-S6K signal at 72 hpa (Figure S6).   In addition, *msxb* and *connexin43* (*cx43*), a molecular marker of proliferating cells [23], expression was downregulated by rapamycin treatment in the regenerative fins (Figure 5D).   Consistent with these *in situ* hybridization results, the number of PCNA-positive cells in both the blastema and epidermis was significantly reduced by rapamycin treatment (Figure 5E,F), as observed before blastema formation (Figure 4).   In contrast to the pre-blastema formation stage, the number of apoptotic cells in both the blastema and epidermis was significantly increased by rapamycin treatment during the blastema formation and regenerative outgrowth stages (Figure 5G,H).   These results suggest that mTORC1 signaling is required for cell proliferation and cell survival during blastema formation and regenerative outgrowth.

mTORC1 signaling is required for the proliferation and differentiation of bony fin ray after 72 hpa

As shown in Figure 2, mTORC1 signaling was specifically activated in the putative differentiating osteoblasts after 72 hpa.   To examine the function of mTORC1 signaling in bony ray formation, the regenerates were treated with rapamycin from 72 to 120 hpa.   Inhibition of mTORC1 signaling was confirmed by the marked reduction of the p-S6K signal at 120 hpa (Figure S7).   The number of BrdU incorporated cells in the Zns-5-positive osteoblasts was significantly reduced by rapamycin treatment (Figure 6B,C).   In addition, the number of Sp7-expressing cells and expression domains of *col10a1a*, which are intermediate markers of skeletogenesis [15], were markedly decreased in the rapamycin-treated fins (Figure 6D,E,F).   In contrast to differentiation markers for skeletogenesis, the number of Runx2-positive osteoblast progenitors was unchanged by rapamycin treatment (Figure 6G,H).   These results suggest that

mTORC1 signaling is required for proliferation and differentiation of the bony fin ray after 72 hpa.

mTORC1 signaling does not regulate autophagy in fin regeneration

A recent study revealed that autophagy is required for zebrafish fin regeneration under the control of MAPK/Erk signaling pathway [24]. Because the mTORC1 signaling pathway is known to inhibit autophagy [7,8], we examined whether autophagy was affected by inhibition of mTORC1 signaling during fin regeneration. As determined using a GFP-microtubule-associated protein 1 light chain 3 isoform (GFP-LC3) transgenic line, autophagy was markedly upregulated from 1 to 4 days post amputation (dpa) [24]. Using an LC3B antibody, we detected LC3 in the wound epidermis at 24 hpa, and by 72 hpa, LC3 localization in the wound epidermis was maintained (Figure S8). Moreover, LC3 protein level and localization were not affected by rapamycin treatment (Figure S8), suggesting that the mTORC1 signaling pathway does not regulate fin regeneration via autophagy.

IGF-1 receptor (IGF-1R)/PI3K and Wnt signaling pathways regulate mTORC1/S6K in fin regeneration

It is well known that the mTORC1/S6K pathway is regulated through the receptor tyrosine kinase/PI3K/Akt pathway in cell proliferation and metabolism [7,8]. To examine the upstream signaling pathway regulating mTORC1/S6K signaling in fin regeneration, various inhibitors for IGF, Wnt, Fgf, and ROS signaling pathways were tested from -12 h to 24 hpa or from 24 to 48 hpa, and S6K activation was determined; IGF signaling (LY294002 [25]: a PI3K inhibitor, NVP-ADW742 [26]: a IGF-1 receptor kinase inhibitor), Wnt signaling (IWP-2 [27]: a Wnt/b-catenin signaling inhibitor), Fgf signaling (SU5402 [28]: a Fgf receptor1 inhibitor), MAPK/Erk signaling (U0126 [29]: a MAPK/Erk inhibitor), and ROS signaling (VAS2870 [30]: an inhibitor of NADPH oxidase). No inhibitory effect for S6K activation was observed using SU5402, U0126, or VAS2870, even though fin regeneration was suppressed (Figure S9). However, LY294002, NVP-ADW742, and IWP-2 inhibitor treatment markedly reduced the p-S6K signal in blastema and epidermal cells. The inhibitory effect of LY294002, NVP-ADW742, and IWP-2 on S6K activation was nearly similar to that of rapamycin during fin regeneration (Figure 7). These results suggest that both IGF-1R/PI3K and

Wnt pathways activate mTORC1 in blastema and epidermal cells during zebrafish caudal fin regeneration.

Discussion

Based on the localization of p-S6K, we show the spatiotemporal distributions of cells in which mTORC1 signaling is activated during fin regeneration (Figure 1). Weak p-S6K fluorescent signals were observed in the intra-ray cells and epidermis as early as 6 hpa. Further, the p-S6K-positive cells were found to be distributed in locations proximal to the amputation plane by 36 hpa, indicating that mTORC1 is one of the earliest signaling in fin regeneration, which is reminiscent of other signaling pathways such as Wnt, Fgf, retinoic acid, and Activin [2,9,10]. We also show that mTORC1 signaling is active in proliferative blastema cells, wound epidermal cells, and osteoblasts during blastema formation and regenerative outgrowth (after 24 hpa) (Figure 2). Inhibition of mTORC1 signaling from 24 to 72 hpa suppresses proliferation of these cells through the inhibition of S6K activation (Figure 5,S6). These results suggest that mTORC1 signaling is continuously required for cellular proliferation during the blastema formation and regenerative outgrowth stages via protein synthesis.

It is well established that mTORC1 signaling activates anabolic processes, including the synthesis of proteins, nucleotides, and lipids, and, as a result, these processes promote cell growth and proliferation [7,8,31]. Protein and nucleotide syntheses are controlled through the activation of S6K, and lipid synthesis is promoted by activating sterol regulatory element binding proteins in an S6K-dependent or -independent manner [8,31]. Based on these findings, the p-S6K-positive cells observed in regenerating fins appear to be in a higher metabolic state that is stimulated by a wound signal. It would be significant to isolate and analyze these cells under high metabolic conditions during fin regeneration.

A recent paper demonstrated that zebrafish caudal fin regeneration is slightly inhibited by rapamycin treatment from 0 to 35 dpa [32]. However, the inhibitory effect of rapamycin observed was milder than the effect observed in our study. The rapamycin concentration used in this report was lower than that used in the present study (50 nM in a previous report versus 2.4 mM in the present study), which may explain this discrepancy. In addition, while fish were pretreated with rapamycin before amputation (-12 h) in our experiments, no pretreatment was performed in the previous report. In fact, we found that at least 6 h of pretreatment is needed to observe the loss of p-S6K immunostaining. When fish were treated with rapamycin from 0

hpa, the inhibitory effect of rapamycin on fin regeneration was markedly reduced, even when using a 2.4 mM concentration of rapamycin (data not shown). It is likely that these two different experimental conditions may be responsible for the difference observed between our study and the previous report.

A previous report showed that *insulin-like growth factor 2b* (*igf2b*), which is expressed in blastema, activates the IGF signaling pathway in the apical epithelium cells through two receptors, insulin-like growth factor 1a receptor (Igf1ra) and Igf1rb [33]. Pharmacological inhibition using NVP-ADW541 or NVP-ADW742 caused apoptosis in the wound epidermis and blocked blastema formation, indicating that IGF signaling between blastema and wound epidermis is critical for cell survival in the wound epidermis and cell proliferation in the blastema [33]. These results are consistent with some of our results showing that mTORC1 signaling is active in the wound epidermis before blastema formation, and is regulated by the IGF-1R/PI3K signaling pathway. However, two phenotypic differences were observed between mTORC1 and IGF-1R inhibition during fin regeneration. One is that cell death was significantly increased in the wound epidermis by IGF-1R inhibition at 24 hpa [33], but not by rapamycin treatment from -12 h to 18 hpa (Figure 4). Because the IGF signaling is one of upstream signaling leading to mTORC1/S6K pathway, the other signaling pathways might be involved in the wound epidermis survival. The second is that activation of mTORC1 based on p-S6K localization was observed not only in the wound epidermis, but also in intra-ray cells as early as 6 hpa. It is possible that, in intra-ray cells, mTORC1 signaling is activated through IGF-1Rs, other than Igf1ra and Igf1rb.

In addition to IGF-1R/PI3K signaling, we also found that Wnt signaling controls mTORC1 activation in both blastema and epidermal cells during fin regeneration by using IWP-2 (Figure 7). It has already been shown that Wnt signaling directly activates mTORC1 through the inhibition of glycogen synthase kinase 3 and tuberous sclerosis 1/2 in zebrafish and mice [34], as well as in mammalian cell lines [35]. In zebrafish caudal fin regeneration, Wnt/b-catenin signaling indirectly regulates the proliferation of blastema cells, patterning of epidermis, and differentiation and patterning of bone, mediated through many signaling pathways such as Activin, Notch, Fgf, retinoic acid, Hedgehog, IGF, and Bmp [10]. Because mTORC1 signaling could be mediated directly or indirectly through IGF signaling regulated by Wnt/b-catenin signaling, further detailed investigations are needed to elucidate the hierarchical

relationship and crosstalk between IGF-1R/PI3K/mTORC1 and other signaling pathways downstream of Wnt/b-catenin during fin regeneration.

Materials and Methods

Zebrafish husbandry, fin amputation, drug treatments, and *in vivo* electroporation

All zebrafish experiments were performed under ethical approval of the Hiroshima University Animal Research Committee (Permit Number: F13-1). Maintenance and caudal fin amputation of adult zebrafish (AB/Tüebingen strain) were performed as described previously [36]. Transgenic zebrafish XIG8A [Tg(*ef1-a:EGFP*)] [21] was used for fin amputation experiments.

During drug treatments, fish were kept in fish water at 28.5 °C and the fish water with drug was replaced daily. 2.4 mM rapamycin (LC Laboratories), 100 nM Torin1 (Calbiochem), 1.2 mM AZD8055 (AdooQ Biosciences), 10 mM LY294002 (Calbiochem), 5 mM NVP-ADW742 (AdooQ Biosciences), 14 mM SU5402 (Calbiochem), 10 mM IWP-2 (Promega), 25 mM U0126 (Promega), and 1 mM VAS2870 (Enzo Life Sciences) were used as specific inhibitors. All were dissolved in DMSO and final DMSO concentration in fish water was 0.1%, except SU5402 (0.17%). The control fish were kept in fish water with 0.1% DMSO.

For MO knockdown experiments, *in vivo* electroporation was performed as described previously [37]. The MO was micro-injected between each bony fin ray and electroporated before fin amputation. We used fluorescent tagged-MO targeted against *raptor* and 5-base mismatch control MO (Gene Tools, Inc.) as following; a raptor MO (5'-ATGGATGGATGGATGCTCACCTATC-3') [19], a 5-mismatch control MO (5'- ATGaATGaATGaATGaTCACaTATC -3', lower case letters indicate mismatch pairs).

Immunohistochemical staining and whole-mount *in situ* hybridization

The amputated fins were fixed in 4% paraformaldehyde in 0.1 M phosphate-buffered saline (PBS) overnight at 4 °C. After fixation, the fins were treated with PBS containing 30% sucrose overnight, and were embedded with Tissue-Tek O.C.T. compound (Sakura Finetek). The embedded fins were frozen and sectioned to 14 mm thickness by using a Leica CM3050S. The sections were dehydrated and rehydrated through a methanol/PBS-0.1% Tween series for 5 min each. After rehydration, the sections were blocked with PBST (PBS and 0.1% Tween20) containing 5% sheep serum for 3 h at room temperature and then incubated in PBST

with primary antibody/antibodies overnight at 4 ˚C.   The following primary antibodies were used: anti-PCNA mouse monoclonal antibody at 1:1000 (Sigma, #P8825) [36]; anti-BrdU rat monoclonal antibody at 1:100 (Abcam, ab6326); phospho-S6 ribosomal protein (Ser240/244) rabbit polyclonal antibody at 1:300 (Cell Signaling, #2215) [38]; anti-Runx2 mouse monoclonal antibody at 1:100 (Sant Cruz Biotechnology, 27-K) [10,11]; anti-Zns-5 mouse monoclonal antibody at 1:300 (a kindly gift from Dr. Ishitani) [14]; anti-Sp7 rabbit polyclonal antibody at 1:1000 (Santa cruz, sc-22536-R) [11]; anti-LC3B rabbit polyclonal antibody at 1:300 (Abcam, ab51520) [39].   The following secondary antibodies were used: Alexa Fluor® 488 goat anti-rabbit IgG antibody at 1:500 (Invitrogen, Life Technologies Corp.); Alexa Fluor® 488 goat anti-rat IgG antibody at 1:500 (Invitrogen, Life Technologies Corp.); Alexa Fluor® 594 goat anti-mouse IgG antibody at 1:500 (Invitrogen, Life Technologies Corp.); Alexa Fluor® 594 goat anti-rabbit IgG Antibody at 1:500 (Invitrogen, Life Technologies Corp.). 4',6-diamidino-2-phenylindole (DAPI) was used for nuclei staining at a concentration of 1:1000.   The images were captured using an Olympus FV1000-D confocal microscope with the same exposure times using the FluoView software.

Whole-mount *in situ* hybridization analyses were performed as described previously [40] with 60 minute proteinase K treatment.

BrdU incorporation assays and cell death detection

BrdU incorporation assays were performed as described previously [36]. Fin-amputated fish were allowed to regenerate in the fish water containing with 50 mg/ml BrdU between 18 to 24 hpa or 108 to 120 hpa.   After incubation, the regenerating fins were cut and BrdU-labeled cells were detected as described previously [36].   For detection of apoptotic cells, we performed TUNEL staining using an *In Situ* Cell Death Detection Kit (Roche Applied Science) according to the manufacture's instruction.

Acknowledgements

References

1. Tanaka EM, Reddien PW: The cellular basis for animal regeneration. Dev Cell 2011, 21(1):172-185.

2. Gemberling M, Bailey TJ, Hyde DR, Poss KD: The zebrafish as a model for complex tissue regeneration. Trends Genet 2013, 29(11):611-620.

3. Nechiporuk A, Keating MT: A proliferation gradient between proximal and msxb-expressing distal blastema directs zebrafish fin regeneration. Development 2002, 129(11):2607-2617.

4. Akimenko MA, Marí-Beffa M, Becerra J, Géraudie J: Old questions, new tools, and some answers to the mystery of fin regeneration. Dev Dyn 2003, 226(2):190-201.

5. Poss KD, Keating MT, Nechiporuk A: Tales of regeneration in zebrafish. Dev Dyn 2003, 226(2):202-210.

6. Grotek B, Wehner D, Weidinger G: Notch signaling coordinates cellular proliferation with differentiation during zebrafish fin regeneration. Development 2013, 140(7):1412-1423.

7. Li J, Kim SG, Blenis J: Rapamycin: One Drug, Many Effects. Cell Metab 2014, 19(3):373-379.

8. Laplante M, Sabatini DM: mTOR signaling in growth control and disease. Cell 2012, 149(2):274-293.

9. Tal TL, Franzosa JA, Tanguay RL: Molecular signaling networks that choreograph epimorphic fin regeneration in zebrafish - a mini-review. Gerontology 2010, 56(2):231-240.

10. Wehner D, Cizelsky W, Vasudevaro MD, Ozhan G, Haase C, Kagermeier-Schenk B, Röder A, Dorsky RI, Moro E, Argenton F et al: Wnt/β-Catenin Signaling Defines Organizing Centers that Orchestrate Growth and Differentiation of the Regenerating Zebrafish Caudal Fin. Cell Rep 2014, 6(3):467-481.

11. Stewart S, Gomez AW, Armstrong BE, Henner A, Stankunas K: Sequential and opposing activities of Wnt and BMP coordinate zebrafish bone regeneration. Cell Rep 2014, 6(3):482-498.

12.   Gauron C, Rampon C, Bouzaffour M, Ipendey E, Teillon J, Volovitch M, Vriz
        S: Sustained production of ROS triggers compensatory proliferation and is
        required for regeneration to proceed. Sci Rep 2013, 3:2084.

13.   Brown AM, Fisher S, Iovine MK: Osteoblast maturation occurs in overlapping
        proximal-distal compartments during fin regeneration in zebrafish. Dev Dyn
        2009, 238(11):2922-2928.

14.   Woods AL, Hall PA, Shepherd NA, Hanby AM, Waseem NH, Lane DP,
        Levison DA: The assessment of proliferating cell nuclear antigen (PCNA)
        immunostaining in primary gastrointestinal lymphomas and its relationship to
        histological grade, S+G2+M phase fraction (flow cytometric analysis) and
        prognosis. Histopathology 1991, 19(1):21-27.

15.   Johnson SL, Weston JA: Temperature-sensitive mutations that cause
        stage-specific defects in Zebrafish fin regeneration. Genetics 1995,
        141(4):1583-1595.

16.   Li N, Felber K, Elks P, Croucher P, Roehl HH: Tracking gene expression during
        zebrafish osteoblast differentiation. Dev Dyn 2009, 238(2):459-466.

17.   Thoreen CC, Kang SA, Chang JW, Liu Q, Zhang J, Gao Y, Reichling LJ, Sim T,
        Sabatini DM, Gray NS: An ATP-competitive mammalian target of rapamycin
        inhibitor reveals rapamycin-resistant functions of mTORC1. J Biol Chem 2009,
        284(12):8023-8032.

18.   Chresta CM, Davies BR, Hickson I, Harding T, Cosulich S, Critchlow SE,
        Vincent JP, Ellston R, Jones D, Sini P et al: AZD8055 is a potent, selective, and
        orally bioavailable ATP-competitive mammalian target of rapamycin kinase
        inhibitor with in vitro and in vivo antitumor activity. Cancer Res 2010,
        70(1):288-298.

19.   Makky K, Tekiela J, Mayer AN: Target of rapamycin (TOR) signaling controls
        epithelial morphogenesis in the vertebrate intestine. Dev Biol 2007,
        303(2):501-513.

20.   Akimenko MA, Johnson SL, Westerfield M, Ekker M: Differential induction of
        four msx homeobox genes during fin development and regeneration in zebrafish.
        Development 1995, 121(2):347-357.

21.   Urasaki A, Morvan G, Kawakami K: Functional dissection of the Tol2
        transposable element identified the minimal cis-sequence and a highly repetitive

sequence in the subterminal region essential for transposition. Genetics 2006, 174(2):639-649.

22. Thummel R, Burket CT, Hyde DR: Two different transgenes to study gene silencing and re-expression during zebrafish caudal fin and retinal regeneration. ScientificWorldJournal 2006, 6 Suppl 1:65-81.

23. Hoptak-Solga AD, Nielsen S, Jain I, Thummel R, Hyde DR, Iovine MK: Connexin43 (GJA1) is required in the population of dividing cells during fin regeneration. Dev Biol 2008, 317(2):541-548.

24. Varga M, Sass M, Papp D, Takács-Vellai K, Kobolak J, Dinnyés A, Klionsky DJ, Vellai T: Autophagy is required for zebrafish caudal fin regeneration. Cell Death Differ 2014, 21(4):547-556.

25. Vlahos CJ, Matter WF, Hui KY, Brown RF: A specific inhibitor of phosphatidylinositol 3-kinase, 2-(4-morpholinyl)-8-phenyl-4H-1-benzopyran-4-one (LY294002). J Biol Chem 1994, 269(7):5241-5248.

26. Mitsiades CS, Mitsiades NS, McMullan CJ, Poulaki V, Shringarpure R, Akiyama M, Hideshima T, Chauhan D, Joseph M, Libermann TA et al: Inhibition of the insulin-like growth factor receptor-1 tyrosine kinase activity as a therapeutic strategy for multiple myeloma, other hematologic malignancies, and solid tumors. Cancer Cell 2004, 5(3):221-230.

27. Chen B, Dodge ME, Tang W, Lu J, Ma Z, Fan CW, Wei S, Hao W, Kilgore J, Williams NS et al: Small molecule-mediated disruption of Wnt-dependent signaling in tissue regeneration and cancer. Nat Chem Biol 2009, 5(2):100-107.

28. Mohammadi M, McMahon G, Sun L, Tang C, Hirth P, Yeh BK, Hubbard SR, Schlessinger J: Structures of the tyrosine kinase domain of fibroblast growth factor receptor in complex with inhibitors. Science 1997, 276(5314):955-960.

29. Favata MF, Horiuchi KY, Manos EJ, Daulerio AJ, Stradley DA, Feeser WS, Van Dyk DE, Pitts WJ, Earl RA, Hobbs F et al: Identification of a novel inhibitor of mitogen-activated protein kinase kinase. J Biol Chem 1998, 273(29):18623-18632.

30. ten Freyhaus H, Huntgeburth M, Wingler K, Schnitker J, Bäumer AT, Vantler M, Bekhite MM, Wartenberg M, Sauer H, Rosenkranz S: Novel Nox inhibitor

VAS2870 attenuates PDGF-dependent smooth muscle cell chemotaxis, but not proliferation. Cardiovasc Res 2006, 71(2):331-341.

31. Shimobayashi M, Hall MN: Making new contacts: the mTOR network in metabolism and signalling crosstalk. Nat Rev Mol Cell Biol 2014, 15(3):155-162.

32. Kujawski S, Lin W, Kitte F, Börmel M, Fuchs S, Arulmozhivarman G, Vogt S, Theil D, Zhang Y, Antos CL: Calcineurin regulates coordinated outgrowth of zebrafish regenerating fins. Dev Cell 2014, 28(5):573-587.

33. Chablais F, Jazwinska A: IGF signaling between blastema and wound epidermis is required for fin regeneration. Development 2010, 137(6):871-879.

34. Valvezan AJ, Huang J, Lengner CJ, Pack M, Klein PS: Oncogenic mutations in adenomatous polyposis coli (Apc) activate mechanistic target of rapamycin complex 1 (mTORC1) in mice and zebrafish. Dis Model Mech 2014, 7(1):63-71.

35. Inoki K, Ouyang H, Zhu T, Lindvall C, Wang Y, Zhang X, Yang Q, Bennett C, Harada Y, Stankunas K et al: TSC2 integrates Wnt and energy signals via a coordinated phosphorylation by AMPK and GSK3 to regulate cell growth. Cell 2006, 126(5):955-968.

36. Hirose K, Shimoda N, Kikuchi Y: Transient reduction of 5-methylcytosine and 5-hydroxymethylcytosine is associated with active DNA demethylation during regeneration of zebrafish fin. Epigenetics 2013, 8(9):899-906.

37. Hyde DR, Godwin AR, Thummel R: In vivo electroporation of morpholinos into the regenerating adult zebrafish tail fin. J Vis Exp 2012(61).

38. Kim SH, Kowalski ML, Carson RP, Bridges LR, Ess KC: Heterozygous inactivation of tsc2 enhances tumorigenesis in p53 mutant zebrafish. Dis Model Mech 2013, 6(4):925-933.

39. Boglev Y, Badrock AP, Trotter AJ, Du Q, Richardson EJ, Parslow AC, Markmiller SJ, Hall NE, de Jong-Curtain TA, Ng AY et al: Autophagy induction is a Tor- and Tp53-independent cell survival response in a zebrafish model of disrupted ribosome biogenesis. PLoS Genet 2013, 9(2):e1003279.

40. Westerfield M: The zebrafish book. Eugene: University of Oregon Press; 1995.

Figures
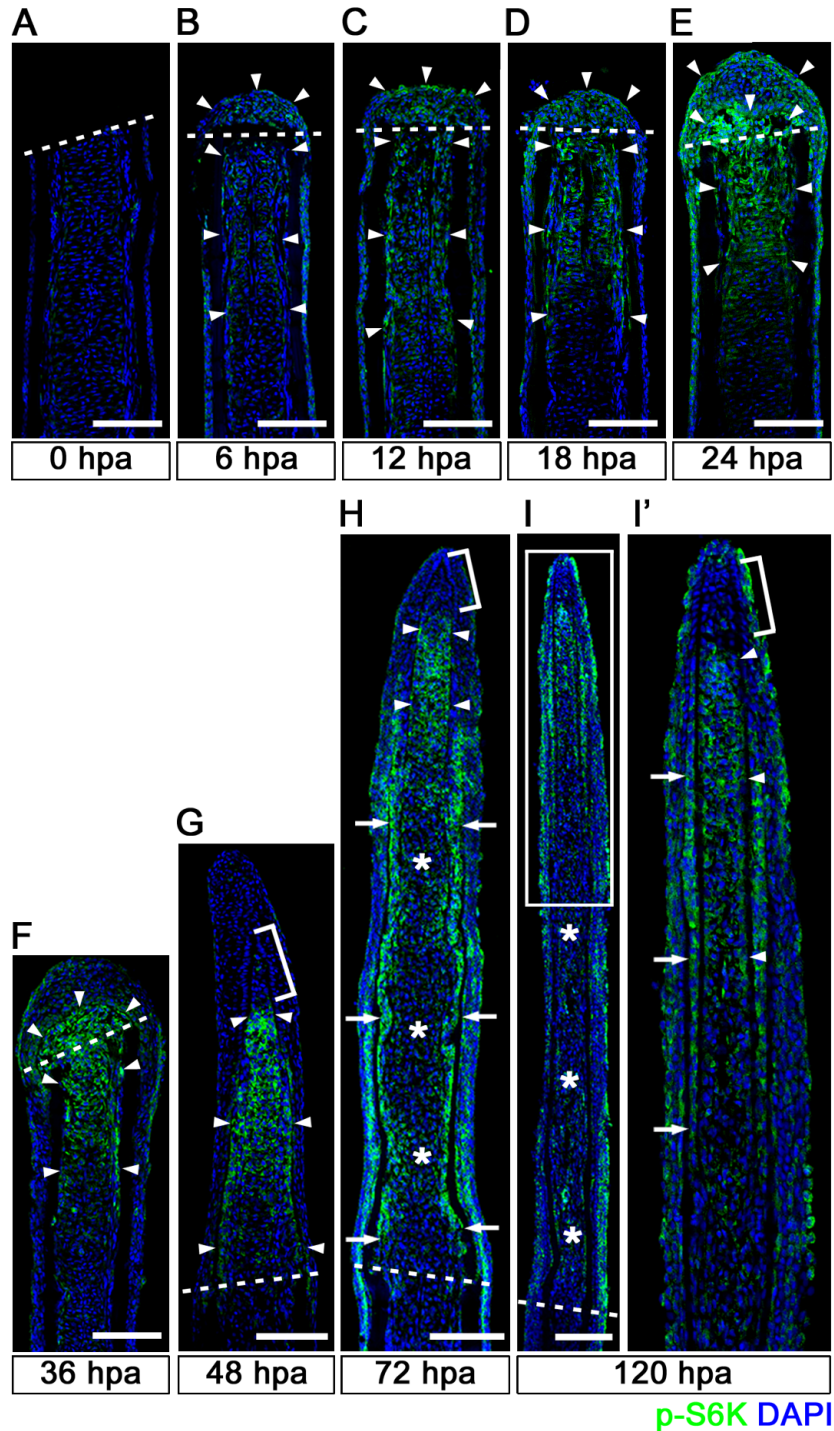
**Figure 1 Spatiotemporal activation of S6K during zebrafish fin regeneration**

(A-I') Longitudinal sections of wild-type fin regenerates that were immunohistochemically stained with an antibody against p-S6K (green) at 0 (A), 6 (B),

12 (C), 18 (D), 24 (E), 36 (F), 48 (G), 72 (H), and 120 (I,I') hpa (0 hpa, n=3; 6 hpa, n=4; 12 hpa, n=3; 18 hpa, n=4; 24 hpa, n=5; 36 hpa, n=4; 48 hpa, n=3; 72 hpa, n=4; 120 hpa, n=3). The boxed area in I is enlarged in I'. DAPI fluorescent signal (blue) indicates the presence of nuclei. Dashed white lines indicate the amputation plane. The p-S6K fluorescent signals were barely detectable in the amputated fin at 0 hpa (A). At 6 hpa, p-S6K-positive cells were found in both intra-ray and epidermal cells (arrowheads in B), and the number of p-S6k-positive cells increased by 24 hpa (arrowheads in C, D, and E). Although p-S6K-positive cells were found in both the blastema and intra-ray region adjacent to and proximal to the amputation plane at 36 hpa (arrowheads in F), p-S6K-positive cells were mainly detected in the blastema at 48 hpa (arrowheads in G). At 72 and 120 hpa, p-S6K-positive cells were observed in the bilateral strip regions (arrows in H and I'), in the putative proximal medial blastema (arrowheads in H and I'), and in the wound epidermis, but not in the putative differentiated blastema cells (asterisks in H and I). Brackets indicate the p-S6K-negative cells in the tip of the putative proximal medial blastema domain and putative distal blastema (G,H,I'). It should be noted that both p-S6K and DAPI fluorescent signals did not overlap, as p-S6K and genomic DNA (DAPI specifically stains double-strand DNA) are localized in the cytosol and nucleus, respectively. Scale bars: 100 mm.
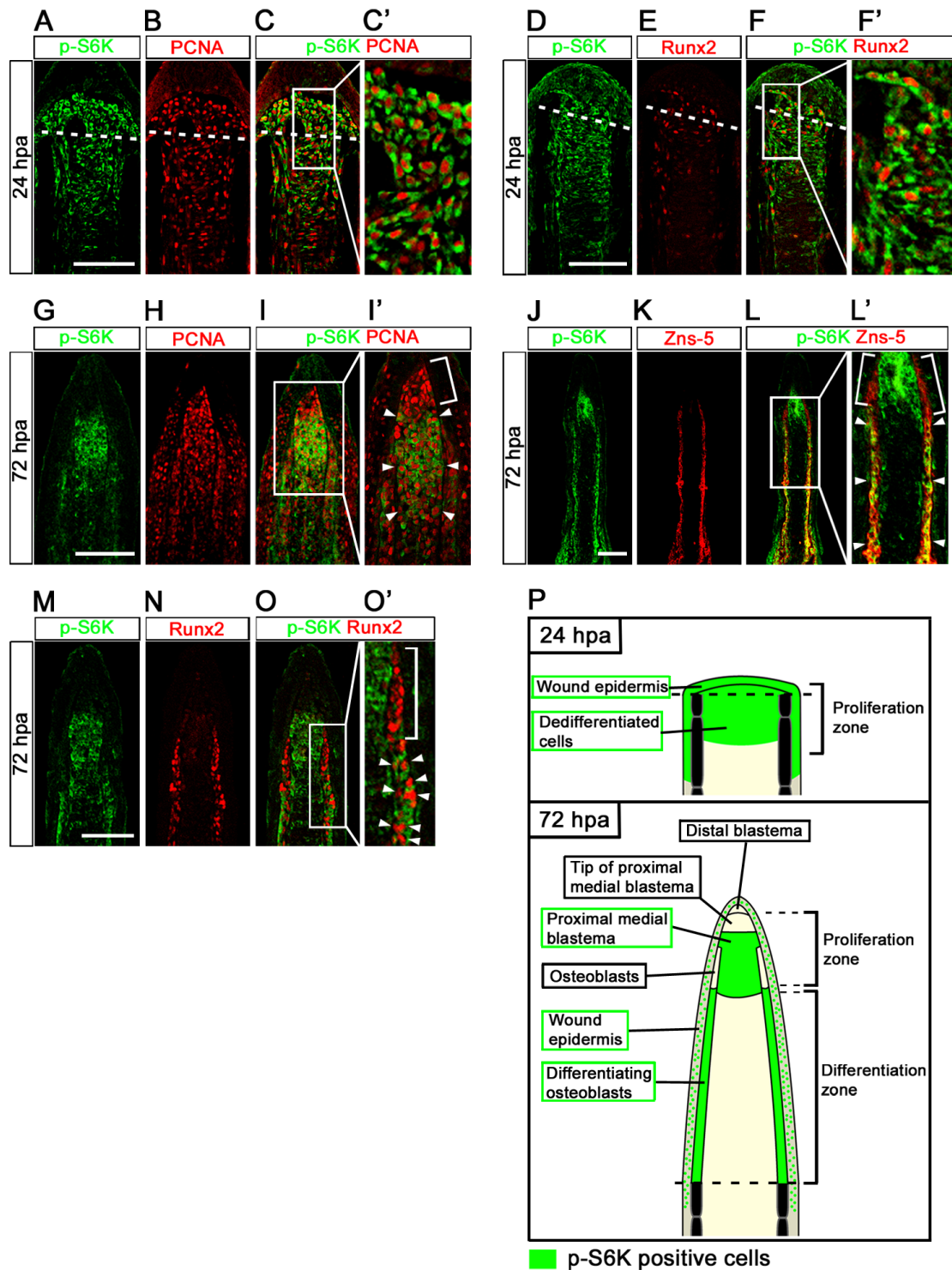
Figure 2 Distributions of S6K-positive cells and proliferative cells at 24 and 72 hpa
(A-F') Longitudinal sections of wild-type fin regenerates that were co-immunohistochemically stained with antibodies against p-S6K (green) and PCNA (red) (A-C', n=3) or p-S6K (green) and Runx2 (red) (D-F', n=3) at 24 hpa.   p-S6K

positive cells were PCNA- or Runx2-positive at 24 hpa (C',F').   The boxed areas in C and F are enlarged in C' and F', respectively.   Dashed white lines indicate the amputation planes.   (G-O') Longitudinal sections of wild-type fin regenerates that were co-immunostained with antibodies against p-S6K (green) and PCNA (red) (G-I', n=5), p-S6K (green) and Zns-5 (red) (J-L', n=3), or p-S6K (green) and Runx2 (red) (M-O', n=4) at 72 hpa.   PCNA-positive cells were p-S6K-positive in the putative proximal medial blastema domain (arrowheads in I'), but not in the tip of the putative proximal medial blastema domain (a bracket in I').   Zns-5- or Runx2-positive cells in the proximal lateral blastema were also p-S6K-positive (arrowheads in L' and O'), but cells in the distal region of the lateral blastema were not (brackets in L' and O').   It should be noted that both p-S6K and PCNA or Runx2 fluorescent signals did not overlap, because p-S6K and PCNA or Runx2 are localized in the cytosol and nucleus, respectively.   Scale bars: 100 mm.   (P) Cartoon summarizing the anatomical structures of fin regenerates in longitudinal cross-sections and localization of p-S6K-positive cells in the fin regenerates at 24 and 72 hpa.   Dashed lines indicate the amputation planes.
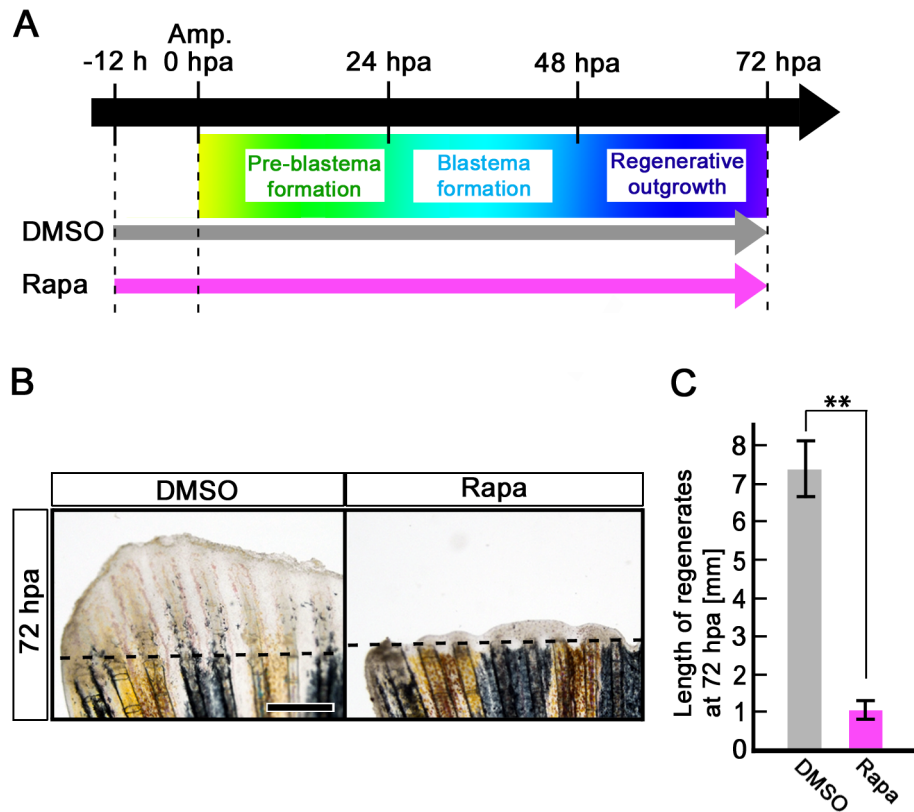
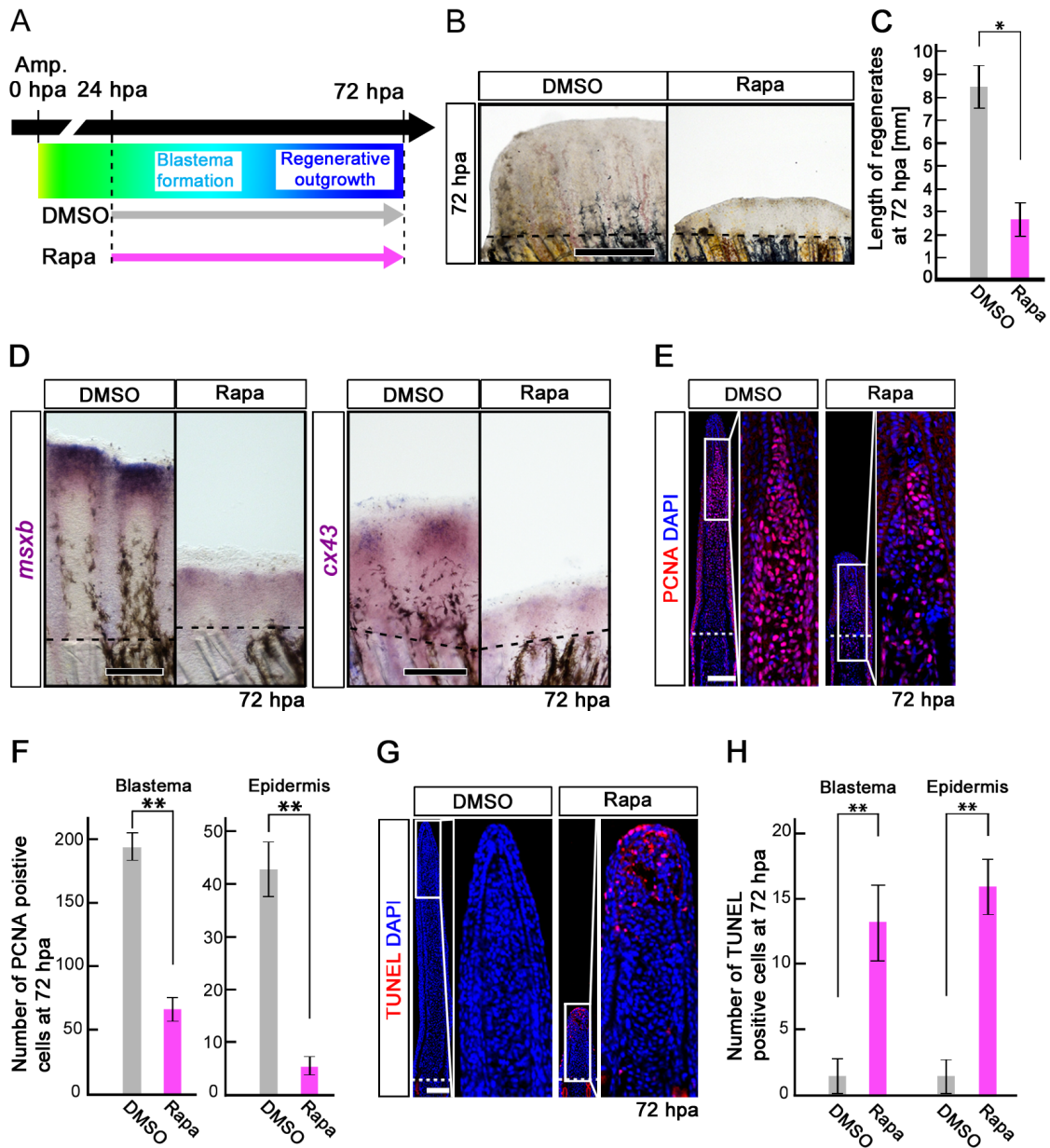**Figure 3 Rapamycin treatment inhibits fin regeneration until 72 hpa**

(A) Scheme of rapamycin treatment from $-$ 12 h to 72 hpa.   (B,C) Rapamycin treatment significantly inhibited fin regeneration from $-$ 12 h to 72 hpa (pre-blastema formation, blastema formation, and regenerative outgrowth stages), when compared to DMSO treatment.   Dashed lines indicate the amputation planes.   ** $p < 0.01$ by Student's t-test.   Error bars represent the standard error of 4 independent experiments. Scale bars: 500 mm in B.
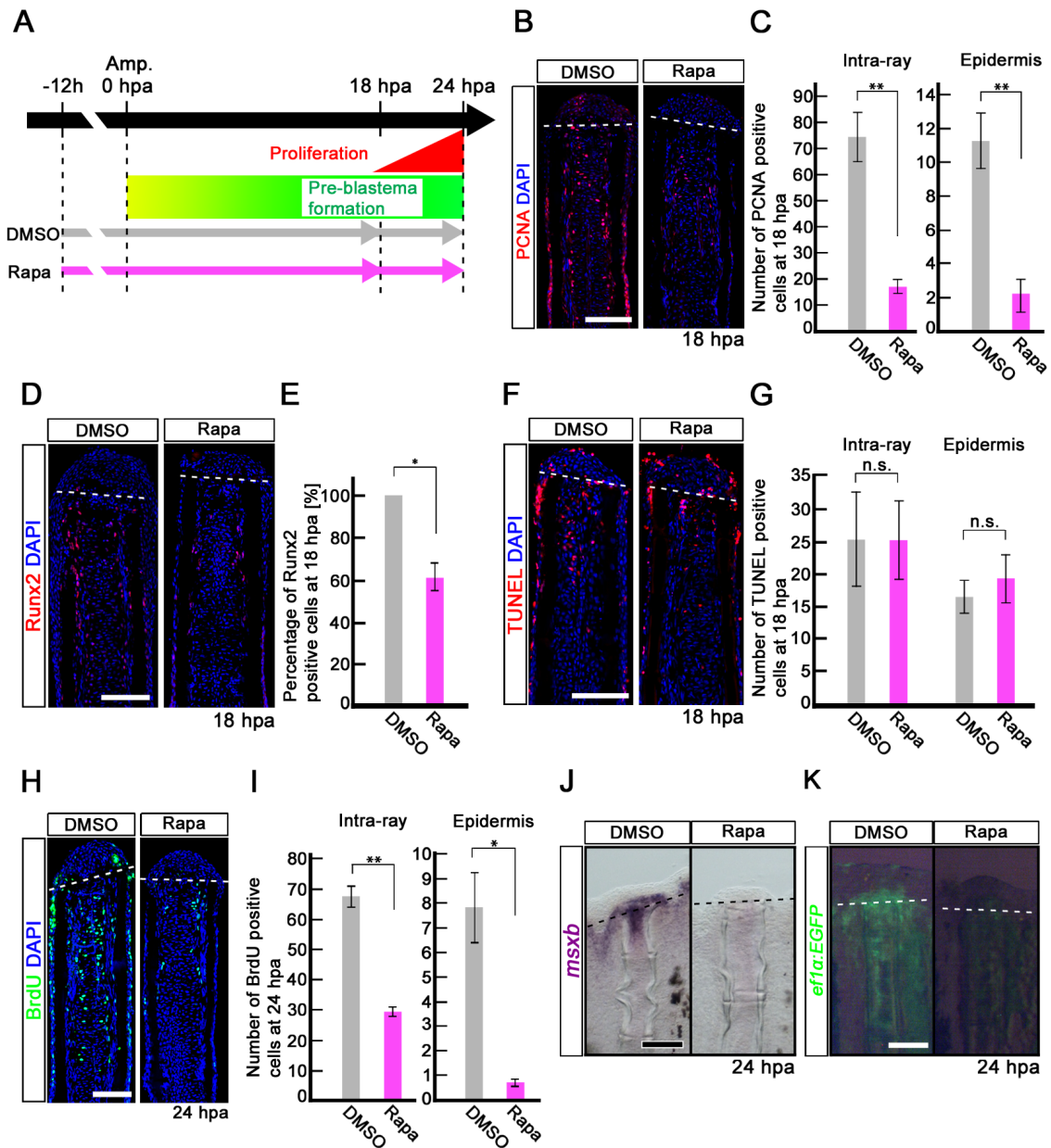
Figure 4 Rapamycin treatment inhibits proliferation of intra-ray and epidermal cells, but not apoptosis before blastema formation

(A) Scheme of rapamycin treatment before blastema formation. (B,C) PCNA-stained fin sections and quantification of PCNA-positive cells in the intra-ray and epidermis at 18 hpa. The number of PCNA-positive cells was significantly reduced by rapamycin treatment in both the intra-ray and epidermis at 18 hpa. ** $p < 0.01$ by Student's t-test. Error bars represent the standard error of 5 independent experiments. Scale bars: 100 mm. (D,E) Runx2-stained fin sections and quantification of Runx2-positive cells in the intra-ray. Rapamycin treatment significantly reduced the percentage of
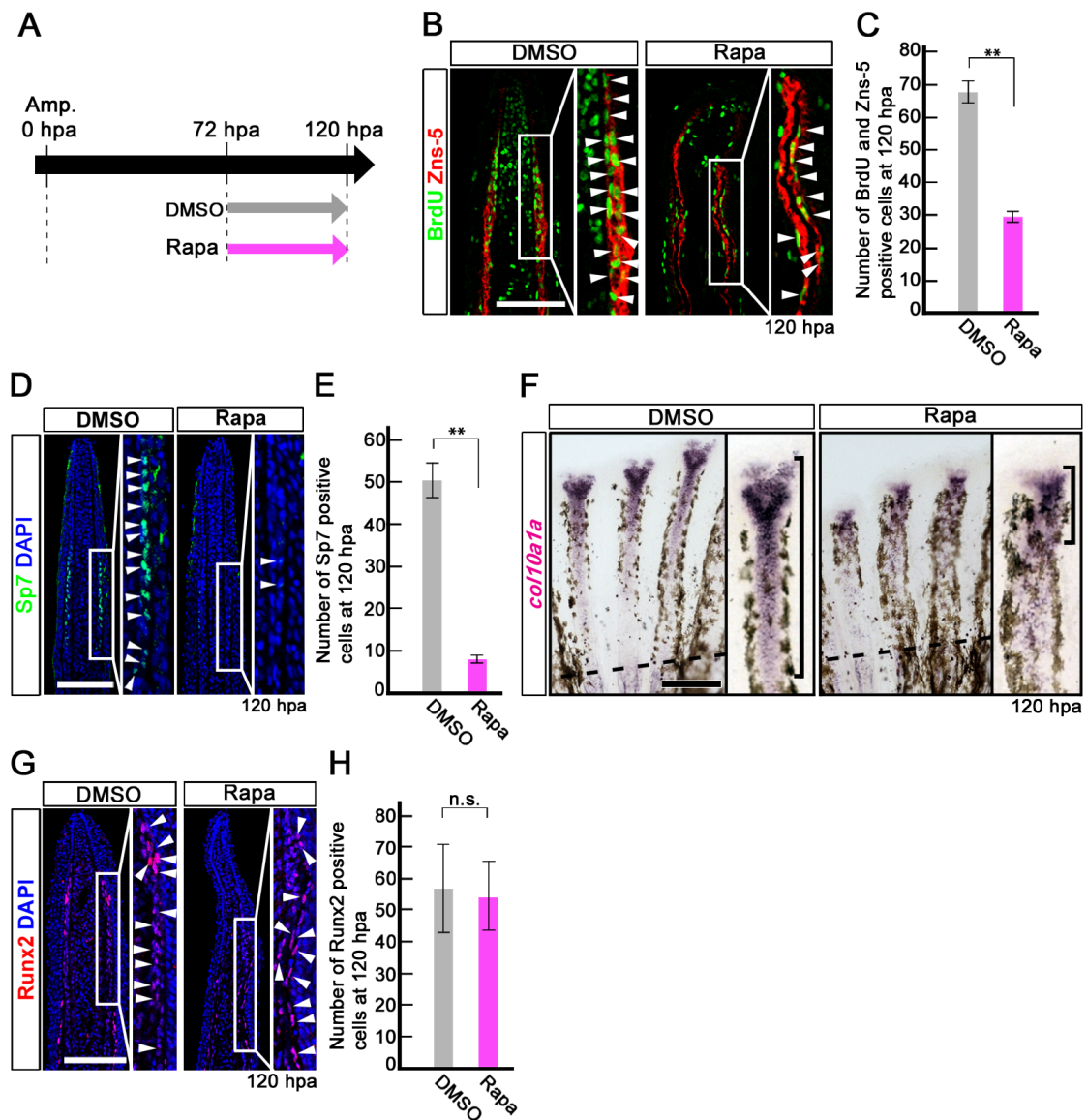
Runx2-positive cells at 18 hpa.   * $p < 0.05$ by Student's *t*-test.   Error bars represent the standard error of 3 independent experiments.   Scale bars: 100 mm.   (F,G) TUNEL-stained fin sections and quantification of TUNEL-positive intra-ray and epidermal cells.   Cell death was not increased in both the intra-ray and epidermis at 18 hpa.   Error bars represent the standard error of 6 independent experiments.   Scale bars: 100 mm.   (H,I) BrdU-stained fin sections and quantification of BrdU-positive cells in the intra-ray and epidermis.   Rapamycin treatment significantly reduced the number of BrdU-positive cells in the intra-ray and epidermis at 24 hpa.   * $p < 0.05$, ** $p < 0.01$ by Student's *t*-test.   Error bars represent the standard error of 3 independent experiments.   Scale bars: 100 mm.   DAPI fluorescent signal (blue) indicates the presence of nuclei (B,D,F,H).   Dashed white lines indicate the amputation planes (B,D,F,H).   (J) Expression of *msxb* was examined by *in situ* hybridization at 24 hpa (n=3).   The *msxb* expression was barely detectable in rapamycin-treated fin regenerates.   Scale bars: 200 mm.   (K) EGFP fluorescence of Tg(*ef1- a;EGFP*) fin regenerates at 24 hpa (n=3).   The EGFP fluorescence was lost in rapamycin-treated fin regenerates.   Scale bars: 200 mm.   Dashed lines indicate the amputation plane (J,K).

Figure 5 Rapamycin treatment inhibits both the proliferation and survival of intra-ray cells during the blastema formation and regenerative outgrowth stages

(A) Scheme of rapamycin treatment during blastema formation and regenerative outgrowth stages.   (B,C) Rapamycin treatment significantly blocked the outgrowth of fin regenerates at 72 hpa.   * $p < 0.05$ by Student's t-test.   Error bars represent the standard error of 4 independent experiments.   Scale bars: 500 mm.   Dashed lines indicate the amputation plane.   (D) Expression of *msxb* and *cx43* was examined by whole-mount *in situ* hybridization at 72 hpa (*msxb*, n=5; *cx43*, n=3).   Rapamycin treatment induced the down-regulation of *msxb* and *cx43* expression.   Scale bars: 200

mm.　Dashed lines indicate the amputation plane.　(E,F) PCNA-stained fin sections and quantification of PCNA-positive cells in the intra-ray and epidermis at 72 hpa. The number of PCNA-positive cells was significantly reduced by rapamycin treatment in both the blastema and epidermis at 72 hpa.　** $p < 0.01$ by Student's t-test.　Error bars represent the standard error of 4 independent experiments.　Scale bars: 100 mm. (G,H) TUNEL-stained fin sections and quantification of TUNEL-positive cells in the intra-ray and epidermis.　Cell death was significantly increased by rapamycin treatment in both the blastema and epidermis at 72 hpa.　** $p < 0.01$ by Student's t-test. Error bars represent the standard error of 4 independent experiments.　Scale bars: 100 mm.　DAPI fluorescent signal (blue) indicates the presence of nuclei (E,G).

Figure 6 Rapamycin treatment inhibits proliferation and differentiation of osteoblasts after 72 hpa

(A) Scheme of rapamycin treatment between 72 and 120 hpa.　(B,C) BrdU and Zns-5 double-stained fin sections and quantification of BrdU and Zns-5 double-positive osteoblasts.　The number of double-positive osteoblasts was significantly reduced by rapamycin treatment at 120 hpa.　** $p < 0.01$ by Student's t-test.　Error bars represent the standard error of 4 independent experiments.　(D,E) Sp7-stained fin sections and quantification of Sp7-positive osteoblasts.　The number of Sp7-positive osteoblasts was significantly reduced by rapamycin treatment at 120 hpa.　DAPI fluorescent signal (blue) indicates the presence of nuclei.　** $p < 0.01$ by Student's t-test.　Error bars

represent the standard error of 4 independent experiments.   Scale bars: 100 mm.   (F) Expression of *col10a1a* was examined by *in situ* hybridization at 120 hpa (n=4). Rapamycin treatment decreased *col10a1a* expression (brackets in F) at 120 hpa. Dashed lines indicate the amputation planes.   Scale bars: 200 mm.   (G,H) Runx2-stained fin sections and quantification of Runx2-positive cells.   The number of Runx2-positive cells was not affected by rapamycin treatment at 120 hpa.   Error bars represent the standard error of 4 independent experiments.   Scale bars: 100 mm.
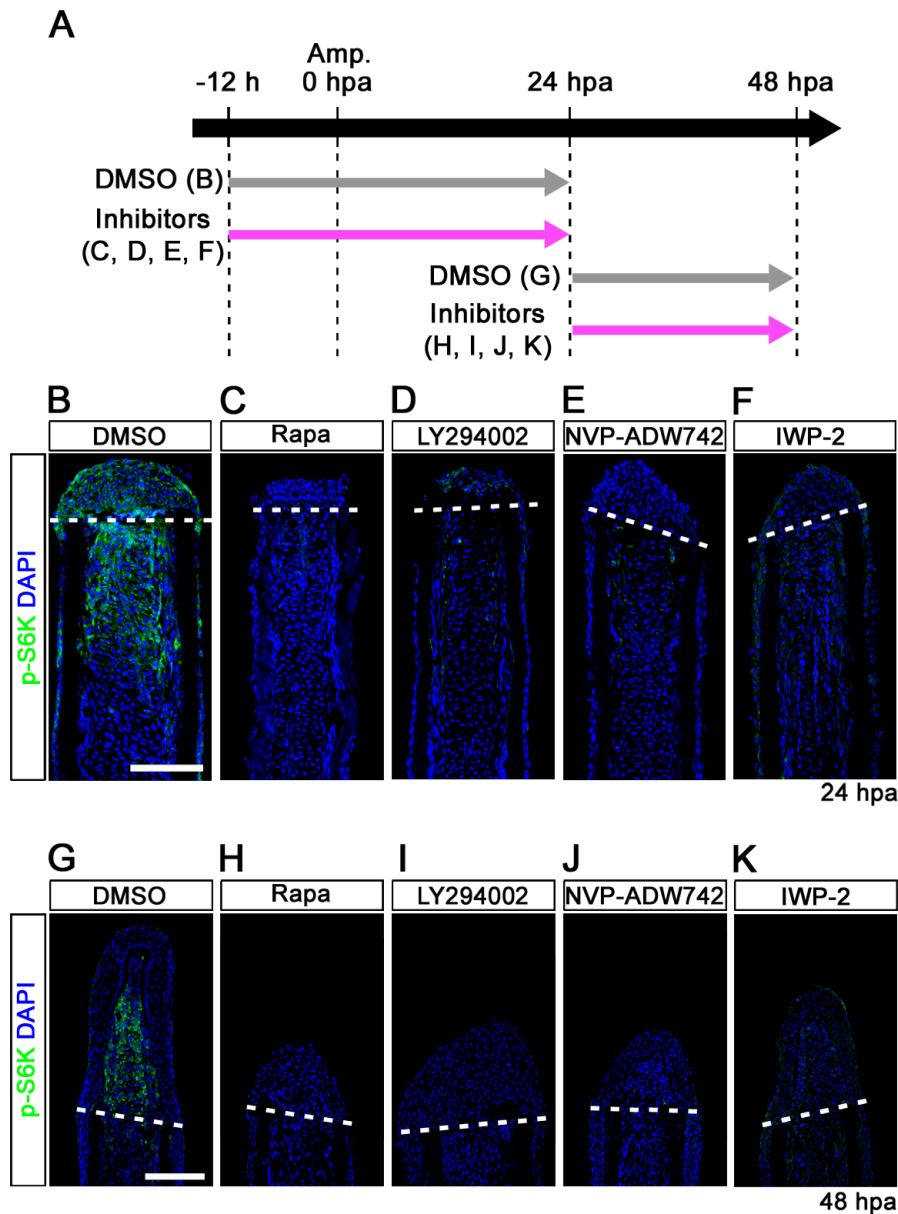
Figure 7 IGF-1R/PI3K and Wnt pathways regulate the activation of mTORC1 during fin regeneration

(A) Scheme of inhibitor treatments of rapamycin, LY294002 (a PI3K inhibitor), NVP-ADW742 (an IGF-1R inhibitor), or IWP-2 (a Wnt/b-catenin inhibitor) during fin regeneration.   (B-I) Longitudinal sections of DMSO or inhibitors treated wild-type fin regenerates that were immunohistochemically stained with an antibody against p-S6K (green) at 24 (DMSO, n=6; Rapa, n=4; LY294002, n=4; NVP-ADW742, n=4; IWP-2, n=5) and 48 hpa (DMSO, n=6; Rapa, n=4; LY294002, n=4; NVP-ADW742, n=4; IWP-2, n=4).   DAPI fluorescent signal (blue) indicates the presence of nuclei.   The

activation of S6K was blocked by LY294002, NVP-ADW742, or IWP-2 treatment. Dashed white lines indicate the amputation planes.   Scale bars: 100 mm.

Supplemental figures
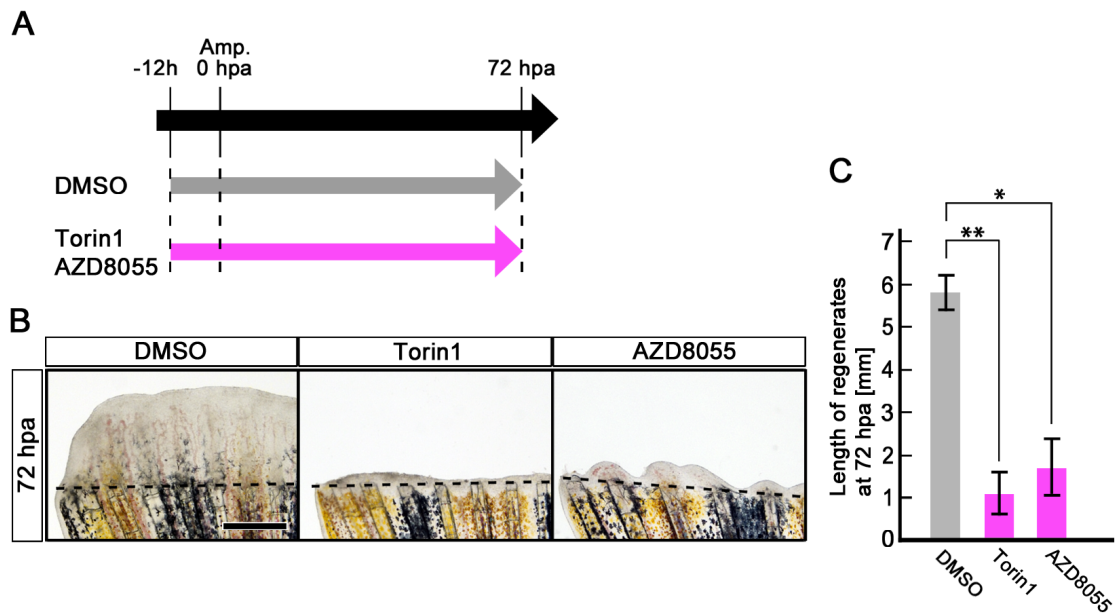
Figure S1. Treatment of Torin1 or AZD8055 inhibits fin regeneration until 72 hpa
(A) Scheme of Torin1 or AZD8055 treatment from – 12 h to 72 hpa.   (B,C) Treatment of both inhibitors significantly inhibited fin regeneration from – 12 h to 72 hpa (pre-blastema formation, blastema formation, and regenerative outgrowth stages), when compared to DMSO treatment.   Dashed lines indicate the amputation planes.   * $p < 0.05$, ** $p < 0.01$ by Student's *t*-test.   Error bars represent the standard error of 4 independent experiments.   Scale bars: 500 mm in B.
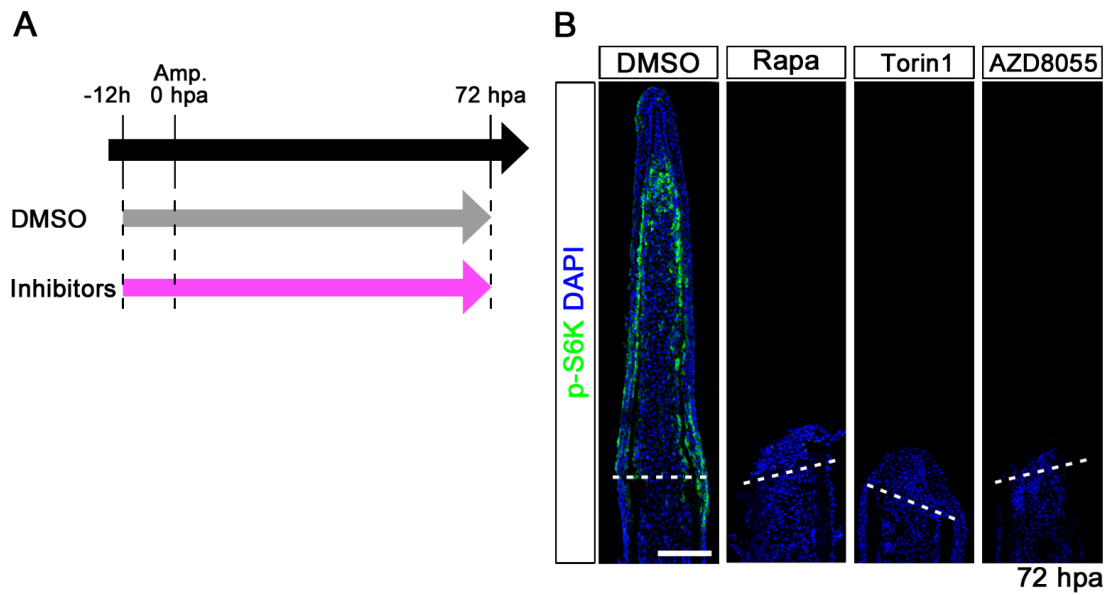
Figure S2. Distributions of p-S6K in rapamycin, Torin1, or AZD8055-treated fin regenerates at 72 hpa

(A) Scheme of rapamycin, Torin1, or AZD8055 treatment from – 12 h to 72 hpa. (B) Longitudinal sections of wild-type fin regenerates that were immunohistochemically stained with an antibody against p-S6K (green) at 72 hpa (DMSO, n=5; Rapa, n=3; Torin1, n=3; AZD8055, n=3). DAPI fluorescent signal (blue) indicates the presence of nuclei. At 72 hpa, the p-S6K fluorescent signal was lost in rapamycin, Torin1, or AZD8055-treated fin regenerates. Dashed white lines indicate the amputation plane. Scale bars: 100 mm.
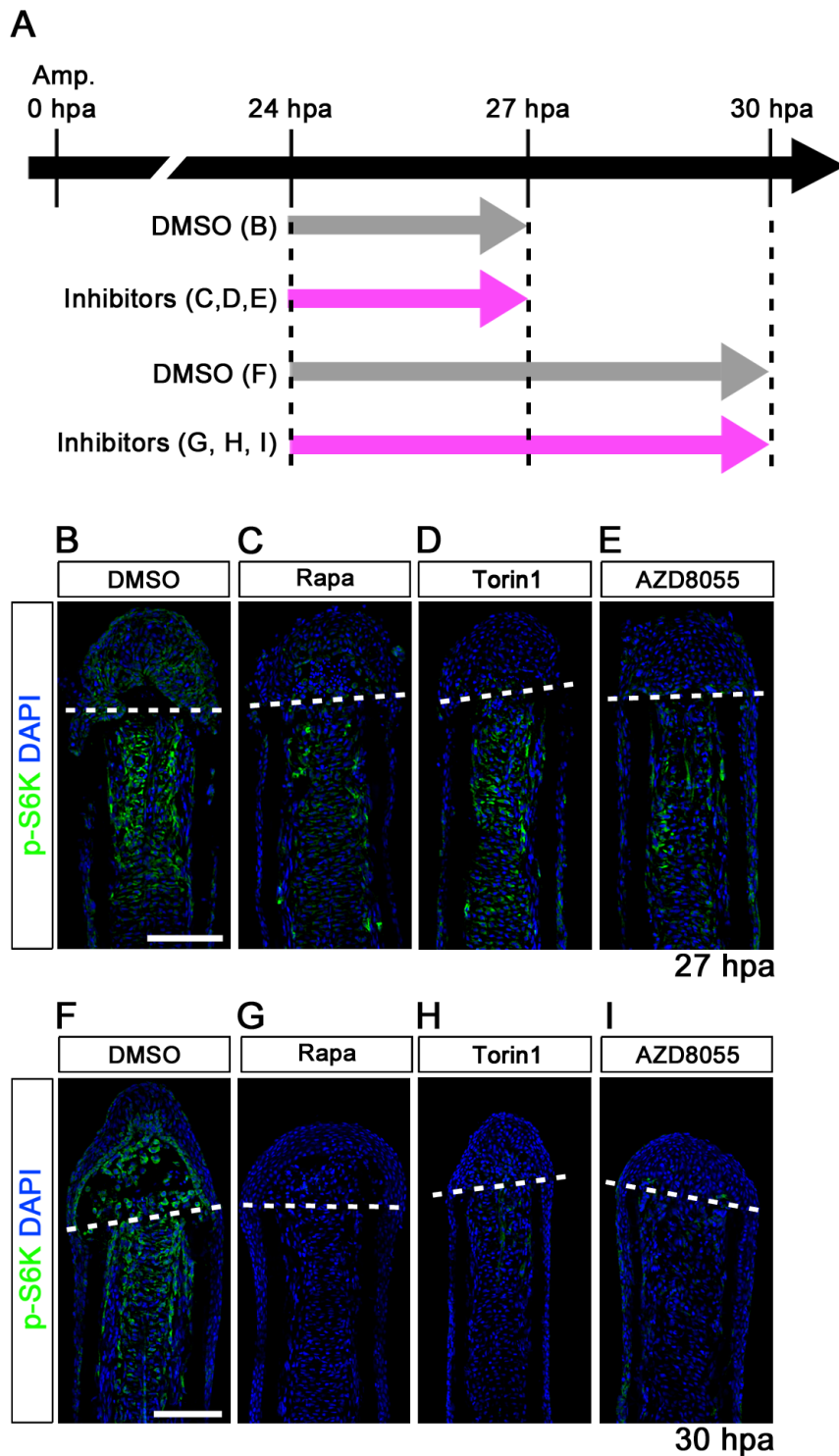
Figure S3. p-S6K signals were markedly reduced by 3 or 6 h treatment with inhibitors (rapamycin, Torin1, and AZD8055)

(A) Scheme of rapamycin, Torin1, or AZD8055 treatment from 24 h to 27 or 30 hpa. (B-I) Longitudinal sections of wild-type fin regenerates that were immunohistochemically stained with an antibody against p-S6K (green) at 27 hpa

(DMSO, n=3; Rapa, n=3; Torin1, n=3; AZD8055, n=3) or 30 hpa (DMSO, n=3; Rapa, n=3; Torin1, n=3; AZD8055, n=3).   DAPI fluorescent signal (blue) indicates the presence of nuclei.   The p-S6K signals were markedly reduced by 3 or 6 h treatment with inhibitors (rapamycin, Torin1, and AZD8055).   Dashed white lines indicate the amputation plane.   Scale bars: 100 mm.
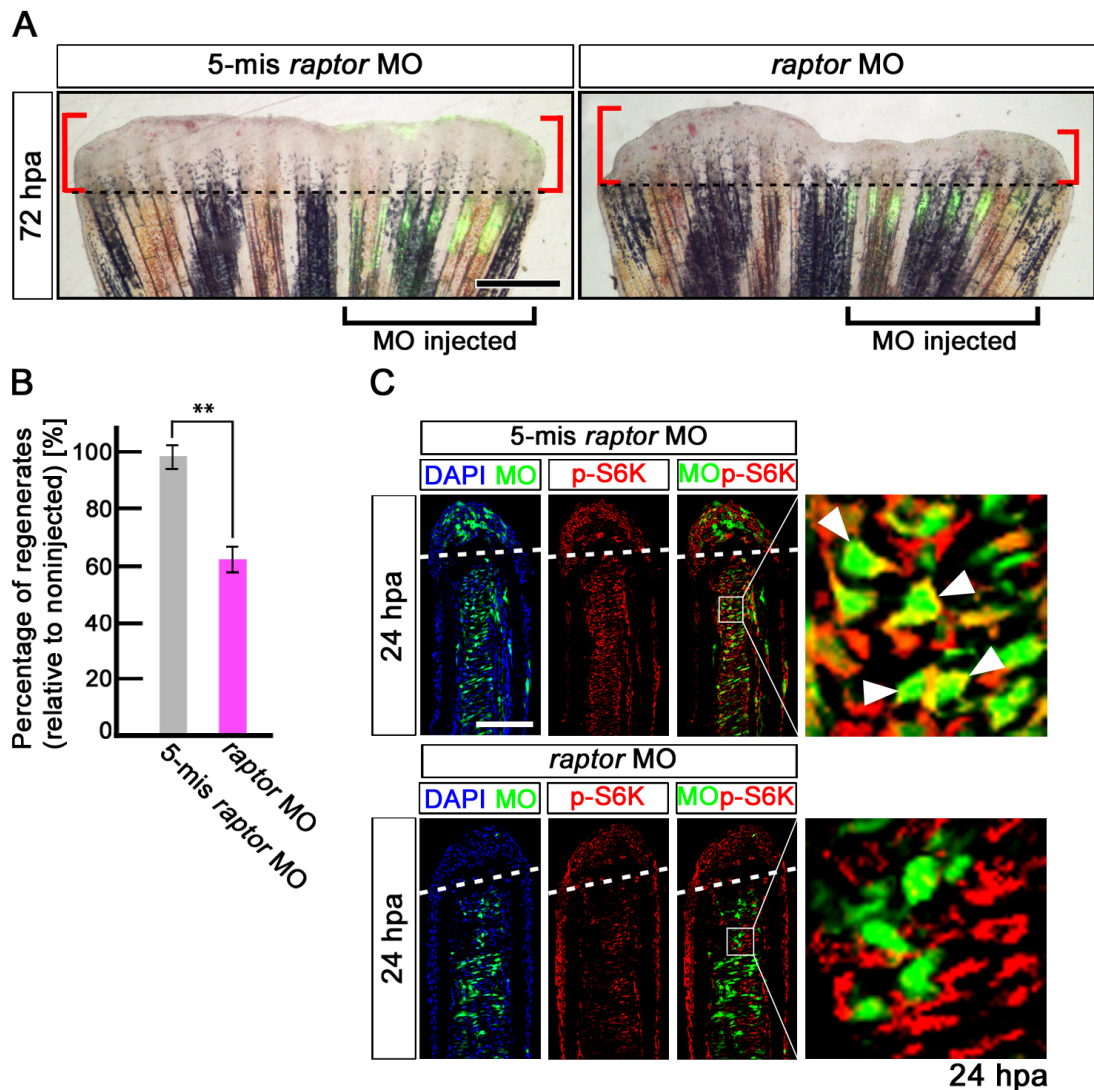
**Figure S4. Fin regeneration and activation of mTORC1 signaling are inhibited by *raptor* knock-down.**

(A,B) Wild-type fin electroporated in the ventral half with fluorescein-labeled MOs at 72 hpa. Fin regeneration was significantly inhibited by *raptor* knock-down. Dashed lines indicate the amputation planes. Scale bars: 500 mm. ** $p < 0.01$ by Student's *t*-test. Error bars represent the standard error of 5 independent experiments. (C) Longitudinal sections of wild-type fin regenerates that were immunostained with antibodies against p-S6K (red) at 24 hpa (5-mismached *raptor* MO, n=5; *raptor* MO, n=5). Green fluorescence indicates the presence of MO in the electroporated cells. Merged views showed that cells incorporated 5-mismached *raptor* MO, but not *raptor* MO, are p-S6K-positive (arrowheads). It should be noted that fluorescent signals of

81

5-mismached *raptor* MO and p-S6K overlap only in the cytosol, because p-S6K are localized in the cytosol, not in the nucleus.   Dashed white lines indicate the amputation planes.   Scale bars: 100 mm.
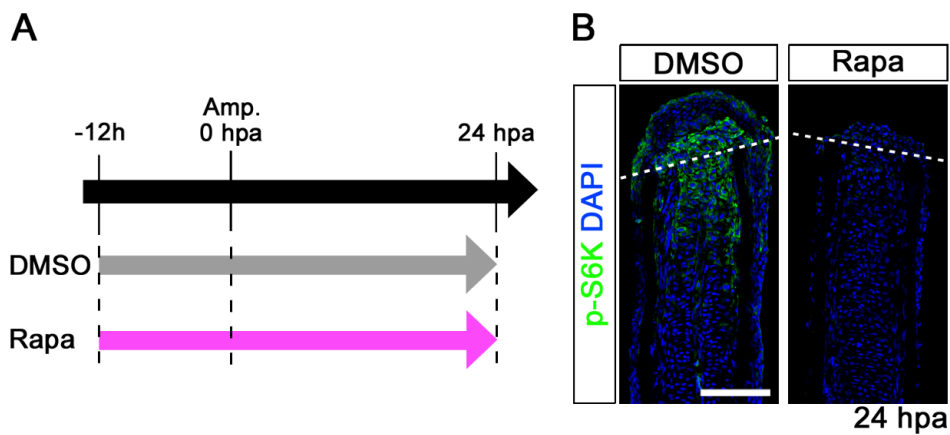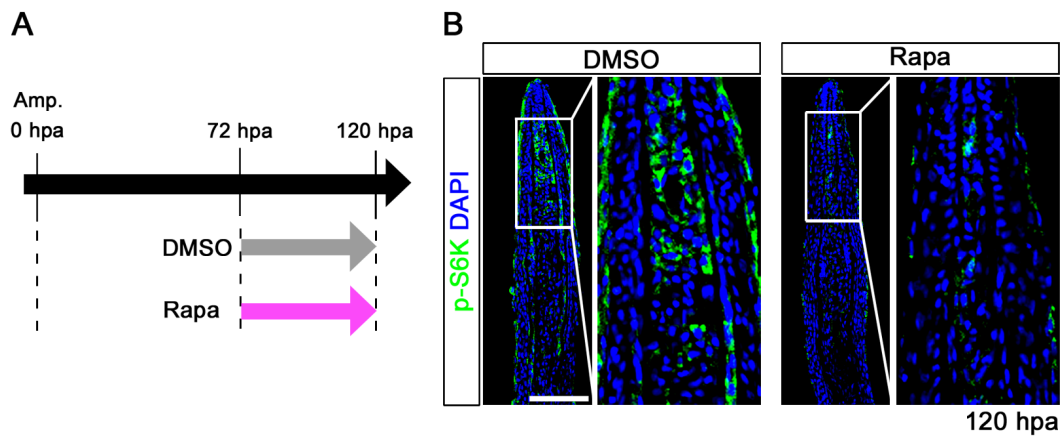
Figure S5. Distributions of p-S6K in rapamycin-treated fin regenerates at 24 hpa
(A) Scheme of rapamycin treatment from – 12 h to 24 hpa.   (B) Longitudinal sections of wild-type fin regenerates that were immunohistochemically stained with an antibody against p-S6K (green) at 24 hpa (DMSO, n=4; Rapa, n=4).   DAPI fluorescent signal (blue) indicates the presence of nuclei.   At 24 hpa, the p-S6K fluorescent signal was lost in rapamycin-treated fin regenerates.   Dashed white lines indicate the amputation plane.   Scale bars: 100 mm.
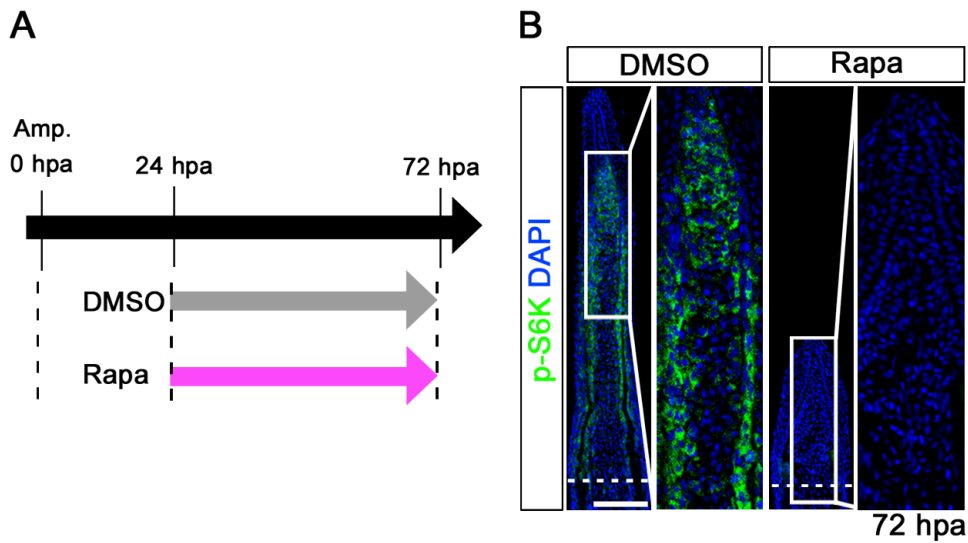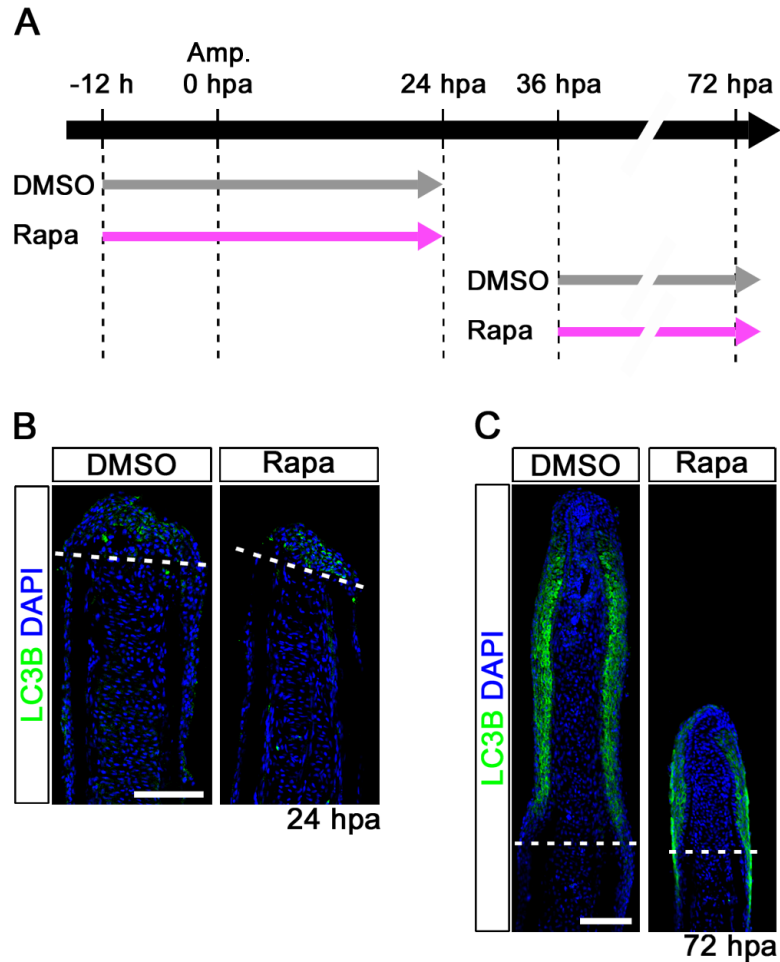
Figure S6. Distributions of p-S6K in fin regenerates treated with rapamycin from 24 to 72 hpa

(A) Scheme of rapamycin treatment from 24 to 72 hpa.   (B) Longitudinal sections of wild-type fin regenerates that were immunohistochemically stained with an antibody against p-S6K (green) at 72 hpa (DMSO, n=5; Rapa, n=5).   DAPI fluorescent signal (blue) indicates the presence of nuclei.   At 72 hpa, the p-S6K fluorescent signal was lost in rapamycin-treated fin regenerates.   Dashed white lines indicate the amputation plane.   Scale bars: 100 mm.

Figure S7. Distributions of p-S6K in fin regenerates treated with rapamycin from 72 to 120 hpa

(A) Scheme of rapamycin treatment from 72 to 120 hpa.　(B) Longitudinal sections of wild-type fin regenerates that were immunohistochemically stained with an antibody against p-S6K (green) at 120 hpa　(DMSO, n=3; Rapa, n=3).　DAPI fluorescent signal (blue) indicates the presence of nuclei.　At 120 hpa, the fluorescent signal of p-S6K was markedly reduced by rapamycin treatment.　Scale bars: 100 mm.

Figure S8. Distributions of LC3B in rapamycin treated fin regenerates

(A) Scheme of rapamycin treatment from -12 to 24 hpa or from 36 to 72 hpa.   (B,C) Longitudinal sections of DMSO or rapamycin treated wild-type fin regenerates that were immunohistochemically stained with an antibody against LC3B (green) at 24 hpa (DMSO, n=4; Rapa, n=4) and 72 hpa (DMSO, n=3; Rapa, n=3).   DAPI fluorescent signal (blue) indicates the presence of nuclei.   LC3B is specifically localized in the wound epidermis at 24 and 72 hpa.   Dashed white lines indicate the amputation planes. Scale bars: 100 mm.
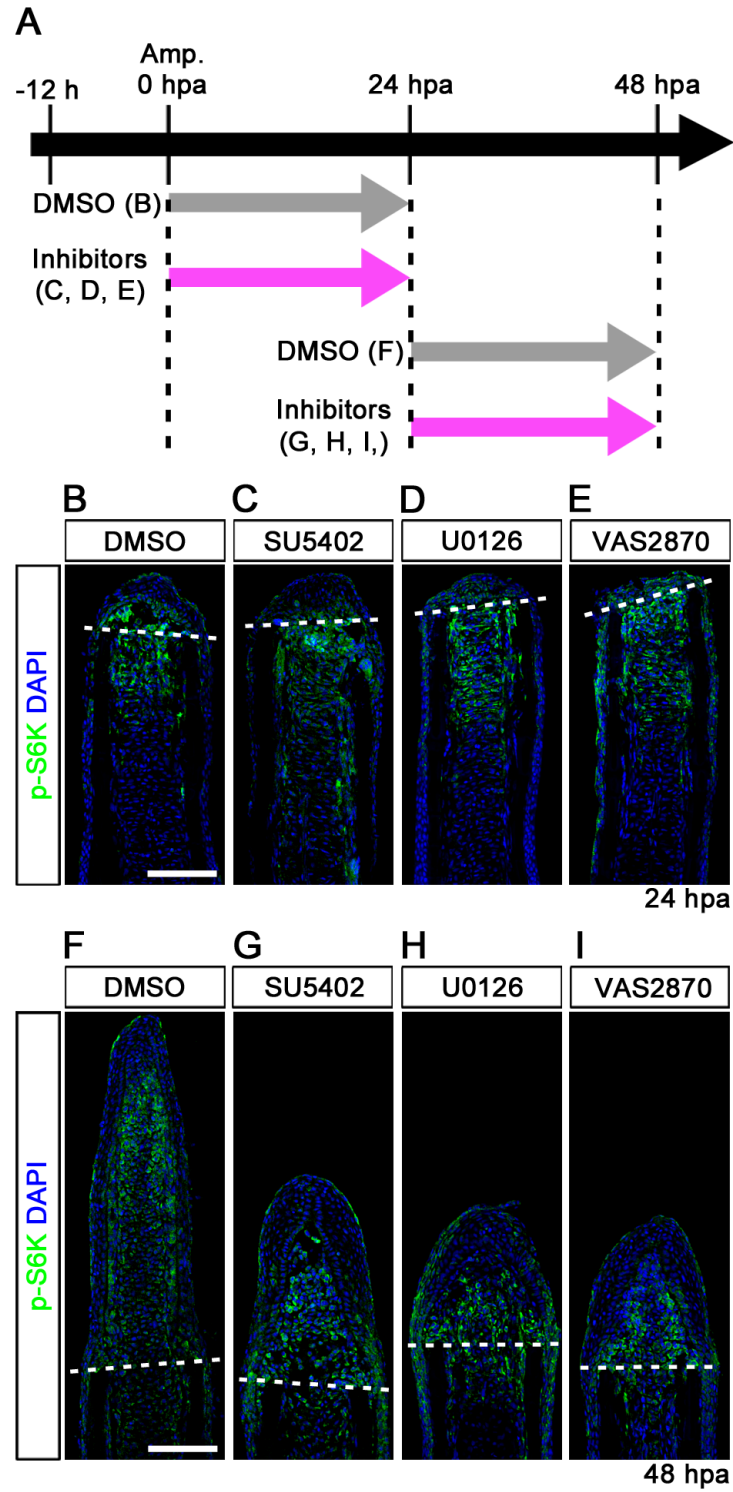
Figure S9. Fgf, MAPK/Erk, and ROS signaling pathways do not regulate the activation of mTORC1 during fin regeneration

(A) Scheme of inhibitor treatments of SU5402 (a Fgf receptor1 inhibitor), U0126 (a MAPK/Erk inhibitor), and VAS2870 (an NADPH oxidase inhibitor: ROS signaling) during fin regeneration. (B-I) Longitudinal sections of DMSO or inhibitors treated wild-type fin regenerates that were immunohistochemically stained with an antibody against p-S6K (green) at 24 or 48 hpa. DAPI fluorescent signal (blue) indicates the presence of nuclei. The p-S6K signals in SU5402-, U0126-, and VAS2870-treated fins were approximately comparable to those in DMSO-treated fins at both 24 hpa (DMSO, n=6; SU5402, n=5; U0126, n=3; VAS2870, n=3) and 48 hpa (DMSO, n=6; SU5402, n=4; U0126, n=3; VAS2870, n=3), even though these inhibitors, at 48 hpa, prevented fin regeneration. Dashed white lines indicate the amputation planes. Scale bars: 100 mm.

Chapter 4. General discussion

General discussion

Although I identified two novel experimental results, reduction of 5mC and 5hmC and activation of mTORC1 during fin regeneration, few reports have been published regarding the relationship between DNA methylation and mTORC1 signaling in regeneration processes. Since reduction of 5mC and 5hmC levels and mTORC1 activation occur in both dedifferentiated cells and blastema cells, the two results may be related. To confirm this possibility, I analyzed 5mC and 5hmC levels following rapamycin treatment during fin regeneration, because initiation of mTORC1 activation occurs prior to reduction of 5mC and 5hmC levels. However, I was unable to observe changes in 5mC and 5hmC levels by mTORC1 inhibition (data not shown). It is also Alternatively, it is possible that the reduction of 5mC and 5hmC levels promotes mTORC1 activation by altering of IGF or Wnt expression, both of which upregulate mTORC1 signaling. Thus, it will be interesting to analyze whether mTORC1 activation is affected by inhibition of 5mC and 5hmC levels reduction, once the DNA demethylation mechanisms has been uncovered.

Considering the function of 5mC and 5hmC levels reduction and mTORC1 activation in blastema, these two processes may cooperatively regulate dedifferentiation in different manners. First, it is a possible that dedifferentiation is caused by 5mC and 5hmC levels reduction. Dedifferentiation is the process by which differentiated cells revert to the precursor state, whereas reprogramming is a process by which differentiated cells revert to the pluripotent state [1]. Thus, dedifferentiation and reprogramming are similar process in terms of reversing cell fate. During reprogramming, erasure of epigenetic marks is necessary for rewriting of epigenetic information. For example, transient reduction of 5mC and 5hmC is observed in mouse preimplantation embryos during reprogramming [2-4]. In addition, DNA methyltransferase inhibitor 5-Aza-deoxycytidine can considerably enhance the reprogramming efficiency of mouse embryonic fibroblasts [5,6]. During regeneration, I speculate that erasure of epigenetic marks is required for dedifferentiation, because differentiated cells must rewrite the epigenetic information for dedifferentiation, as well as reprogramming. Therefore, the reduction of 5mC and 5hmC levels may be process that erases epigenetic memories to facilitate rewriting of epigenetic program in dedifferentiated cells during fin regeneration. Alternatively, it is a possible that

dedifferentiation is caused by mTORC1 activation. Previous reports have indicated that dedifferentiation is regulated by Cyclin D1 or hypoxia inducible factor 1 (Hif1), which are regulated by mTORC1 signaling via translation and gene expression, respectively [7, 8]. It is well known Cyclin D1 is a key factor for cell proliferation [9,10]. During heart regeneration, Cyclin D1 is necessary for promoting cardiomyocyte proliferation [10] and maintains cardiomyocytes in an undifferentiated state by regulating degradation of GATA4 [11]. Proliferative activity and undifferentiated state are the specific characters of dedifferentiated cells. Therefore, Cyclin D1 could regulate dedifferentiation during regeneration. Moreover, Hif1 is a transcription factor induced by hypoxia. Hif1 induces dedifferentiation in hypoxic neuroblastoma [12]. In heart regeneration, hypoxia positively regulates cardiomyocyte dedifferentiation via Hif1α[13]. Therefore, Hif1 could also regulate dedifferentiation, in addition Cyclin D1. Thus, mTORC1 may regulate dedifferentiation through regulation of Cyclin D1 or Hif1α during regeneration. Taken together, my studies indicate that 5mC and 5hmC levels reduction and mTORC1 may cooperatively regulate dedifferentiation in different manners during fin regeneration.

Regeneration is known to be related to cancer via several biological processes [14,15]. For example, oncogenes such as *c-myc* are expressed in regenerating limbs and tails [16], and tumor suppressor genes such as p53 are inactivated in regenerating tissues [17]. In newt limbs, down-regulation of p53 activity has been observed during regeneration, using p53 binding promoter assay, and is necessary for cell proliferation during regeneration [18]. Moreover, injection of a carcinogen into newt limbs induces formation of accessory limbs at the site of injection [19]. These data indicate that cancer and regeneration share common molecular mechanism. Elucidating the relationship may have potential application in regenerative medicine or cancer therapy. In my investigation of reduction of 5mC and 5hmC levels in blastemas, I identified similarities between regeneration and cancer. Previous studies reported that 5mC commonly decreases during the early stage of carcinogenesis [20-22], and that 5hmC decreases in cancer cells at various stages [23-25]. Thus, these data indicate that 5mC and 5hmC decrease in the early stages of carcinogenesis, and only 5hmC remains suppressed in subsequent stages. In blastemas, both 5mC and 5hmC decreased from the pre-blastema formation stage to blastema formation stage, and only 5hmC decreased in following stages. Therefore, in both cancer and blastema cells, 5mC and 5hmC decrease during

the initiation stage and only 5hmC remains suppressed in the following stages. Thus, the reductions of 5mC and 5hmC in cancer and blastema cells may occur via the same mechanism. If so, the data available form cancer studies may advance my study of 5mC and 5hmC level reduction in blastemas, because more advanced data are available from cancer studies, For example, it has already been reported that in cancer, DNA hypomethylation commonly occurrs in repeated DNA sequences, such as long interspersed nuclear element-1 (LINE-1), tandem centrometric satelliteα, juxtacentromeric satellite 2, and the interspersed Alu, using bisulfite sequencing, which connot distinguish between 5mC and 5hmC [26-28]. Although it is remained unclear why and how the DNA hypomethylation occurs, it has been reported that the hypomethylation is linked with tumor progression or the degree of malignancy [20,29]. Satellite 2 hypomethylation has been shown to be significantly correlated with the degree of malignancy in ovarian tumor [29]. Moreover, some studies have indicated that DNA hypomethylation occurs not only in repeated DNA sequences but also in some gene regulatory regions, including the IGF-2 and H19, which contribute to oncogenesis [30, 31]. Therefore, reduction of 5mC and 5hmC levels may plays an important role in blastemas as well as in cancer cells. Studies of cancer may also provide additional results about on the function of reduction of levels of 5mC and 5hmC in blastemas. In addition, mTORC1 activation is commonly detected in cancer cells, and it causes initiation, cell growth, proliferation, and survival of cancer cells [33]. Tuberous sclerosis 1/2 (TSC1/2) are suppressor of mTORC1, and TSC1 or TSC2 knockout significantly induces cancer cells in heterozygous mice [34,35]. In blastemas, mTORC1 signaling is activated and is required for blastema formation, proliferation, and survival. Thus, blastemas resemble to cancer cells with aspect to the function of mTORC1 signaling. Furthermore, TSC2 heterozygous zebrafish mutants also spontaneously induce abdominal tumors in a p53 mutant background [36]. Considering this report on zebrafish mutant [36] and the report on down-regulation of p53 in regenerating newt limbs [18], the circumstances for blastemal formation may also lead to carcinogenesis. However, a regenerating fin has never been reported to develop into cancer. Rather, regeneration is involved in cancer resistance. Salamander limbs into which frog renal tumors have been transplanted can regenerate normal limbs after amputation [37]; furthermore, the renal tumors disappear during regeneration [37]. If

the mechanism that prevents blastemas form causing carcinogenesis can be elucidated, the knowledge may have applications for cancer therapy.

References

1. Jopling C, Boue S, Izpisua Belmonte JC. Dedifferentiation, transdifferentiation and reprogramming: three routes to regeneration. Nat Rev Mol Cell Biol. 2011,12(2):79-89.

2. Gu TP, Guo F, Yang H, Wu HP, Xu GF, Liu W, Xie ZG, Shi L, He X, Jin SG, Iqbal K, Shi YG, Deng Z, Szabó PE, Pfeifer GP, Li J, Xu GL. The role of Tet3 DNA dioxygenase in epigenetic reprogramming by oocytes. Nature. 2011 Sep 4;477(7366):606-10

3. Inoue A, Zhang Y. Replication-dependent loss of 5-hydroxymethylcytosine in mouse preimplantation embryos. Science. 2011, 334(6053):194.

4. Tan L, Shi YG. Tet family proteins and 5-hydroxymethylcytosine in development and disease. Development. 2012, 139(11):1895-902.

5. Seisenberger S, Peat JR, Hore TA, Santos F, Dean W, Reik W. Reprogramming DNA methylation in the mammalian life cycle: building and breaking epigenetic barriers. Philos Trans R Soc Lond B Biol Sci. 2013, 368(1609):20110330.

6. Wernig M, Lengner CJ, Hanna J, Lodato MA, Steine E, Foreman R, Staerk J, Markoulaki S, Jaenisch R. A drug-inducible transgenic system for direct reprogramming of multiple somatic cell types. Nat Biotechnol. 2008, 26(8):916-24.

7. Keyomarsi K, Pardee AB. Redundant cyclin overexpression and gene amplification in breast cancer cells. Proc Natl Acad Sci U S A. 1993, 90(3):1112-6.

8. Toyoda M, Shirato H, Nakajima K, Kojima M, Takahashi M, Kubota M, Suzuki-Migishima R, Motegi Y, Yokoyama M, Takeuchi T. jumonji downregulates cardiac cell proliferation by repressing cyclin D1 expression. Dev Cell. 2003, 5(1):85-97.

9. Nakajima K, Inagawa M, Uchida C, Okada K, Tane S, Kojima M, Kubota M, Noda M, Ogawa S, Shirato H, Sato M, Suzuki-Migishima R, Hino T, Satoh Y, Kitagawa M, Takeuchi T. Coordinated regulation of differentiation and proliferation of embryonic cardiomyocytes by a jumonji (Jarid2)-cyclin D1 pathway. Development. 2011, 138(9):1771-82.

10. Averous J, Fonseca BD, Proud CG. Regulation of cyclin D1 expression by mTORC1 signaling requires eukaryotic initiation factor 4E-binding protein 1. Oncogene. 2008, 27(8):1106-13.

11. Toschi A, Lee E, Gadir N, Ohh M, Foster DA. Differential dependence of hypoxia-inducible factors 1 alpha and 2 alpha on mTORC1 and mTORC2. J Biol Chem. 2008, 283(50):34495-9

12. Fior J. Salamander regeneration as a model for developing novel regenerative and anticancer therapies. J Cancer. 2014, 5(8):715-9.

13. Oviedo NJ, Beane WS. Semin Regeneration: The origin of cancer or a possible cure? Cell Dev Biol. 2009, (5):557-64.

14. Christen B, Robles V, Raya M, Paramonov I, Izpisúa Belmonte JC. Regeneration and reprogramming compared. BMC Biol. 2010, 8:5.

15. Pomerantz JH, Blau HM. Tumor suppressors: enhancers or suppressors of regeneration? Development. 2013, 140(12):2502-12.

16. Yun MH, Gates PB, Brockes JP. Regulation of p53 is critical for vertebrate limb regeneration. Proc Natl Acad Sci U S A. 2013, 110(43):17392-7.

17. BREEDIS C. Induction of accessory limbs and of sarcoma in the Newt (Triturus viridescens) with carcinogenic substances. Cancer Res. 1952, 12(12):861-6.

18. Ehrlich M. DNA hypomethylation in cancer cells. Epigenomics. 2009, 1(2):239-59

19. Gama-Sosa MA, Slagel VA, Trewyn RW, et al. The 5-methylcytosine content of DNA from human tumors. Nucleic Acids Res. 1983;11:6883–6894.

20. Feinberg AP, Vogelstein B. Hypomethylation distinguishes genes of some human cancers from their normal counterparts. Nature. 1983;301:89–92.

21. Jin SG, Jiang Y, Qiu R, Rauch TA, Wang Y, Schackert G, Krex D, Lu Q, Pfeifer GP. 5-Hydroxymethylcytosine is strongly depleted in human cancers but its levels do not correlate with IDH1 mutations. Cancer Res. 2011, 71(24):7360-5.

22. Kraus TF, Globisch D, Wagner M, Eigenbrod S, Widmann D, Münzel M, Müller M, Pfaffeneder T, Hackner B, Feiden W, Schüller U, Carell T, Kretzschmar HA. Low values of 5-hydroxymethylcytosine (5hmC), the "sixth base," are associated with anaplasia in human brain tumors. Int J Cancer. 2012, ;131(7):1577-90.

23. Yang H, Liu Y, Bai F, Zhang JY, Ma SH, Liu J, Xu ZD, Zhu HG, Ling ZQ, Ye D, Guan KL, Xiong Y. Tumor development is associated with decrease of TET gene expression and 5-methylcytosine hydroxylation. Oncogene. 2013, 32(5):663-9.

24. Ehrlich M, Woods CB, Yu MC, Dubeau L, Yang F, Campan M, Weisenberger DJ, Long T, Youn B, Fiala ES, Laird PW. Quantitative analysis of associations between DNA hypermethylation, hypomethylation, and DNMT RNA levels in ovarian tumors. Oncogene. 2006, 25(18):2636-45.

25. Rauch TA, Zhong X, Wu X, Wang M, Kernstine KH, Wang Z, Riggs AD, Pfeifer GP. High-resolution mapping of DNA hypermethylation and hypomethylation in lung cancer. Proc Natl Acad Sci U S A. 2008, 105(1):252-7.

26. Rodriguez J, Vives L, Jordà M, Morales C, Muñoz M, Vendrell E, Peinado MA. Genome-wide tracking of unmethylated DNA Alu repeats in normal and cancer cells. Nucleic Acids Res. 2008, 36(3):770-84.

27. Qu G, Dubeau L, Narayan A, Yu MC, Ehrlich M. Satellite DNA hypomethylation vs. overall genomic hypomethylation in ovarian epithelial tumors of different malignant potential. Mutat Res. 1999, 423(1-2):91-101.

28. Holm TM, Jackson-Grusby L, Brambrink T, Yamada Y, Rideout WM 3rd, Jaenisch R. Global loss of imprinting leads to widespread tumorigenesis in adult mice. Cancer Cell. 2005, (4):275-85.

29. Pogribny IP, Beland FA. DNA hypomethylation in the origin and pathogenesis of human diseases. Cell Mol Life Sci. 2009, 66(14):2249-61.

30. Xu K, Liu P, Wei W. mTOR signaling in tumorigenesis. Biochim Biophys Acta. 2014, 1846(2):638-654.

31. Kobayashi T, Minowa O, Sugitani Y, Takai S, Mitani H, Kobayashi E, Noda T, Hino O. A germ-line Tsc1 mutation causes tumor development and embryonic lethality that are similar, but not identical to, those caused by Tsc2 mutation in mice. Proc Natl Acad Sci U S A. 2001, 98(15):8762-7.

32. Onda H, Lueck A, Marks PW, Warren HB, Kwiatkowski DJ. Tsc2(+/-) mice develop tumors in multiple sites that express gelsolin and are influenced by genetic background. J Clin Invest. 1999, 104(6):687-95.

33. Kim SH, Kowalski ML, Carson RP, Bridges LR, Ess KC. Heterozygous inactivation of tsc2 enhances tumorigenesis in p53 mutant zebrafish. Dis Model Mech. 2013, 6(4):925-33.

34. Borgens RB. Mice regrow the tips of their foretoes. Science. 1982, 217(4561):747-50.

35. Masaki H, Ide H. Regeneration potency of mouse limbs. Dev Growth Differ. 2007 ;49(2):89-98.

Acknowledgement

公表論文

(1) Transient reduction of 5-methylcytosine and 5-hydroxymethylcytosine is associated with active DNA demethylation during regeneration of zebrafish fin.

Kentaro Hirose, Nobuyoshi Shimoda, and Yutaka Kikuchi,

Epigenetics. 2013; 8(9): 899–906.

(2) Mechanistic target of rapamycin complex 1 signaling regulates cell proliferation, cell survival, and differentiation in regenerating zebrafish fins

Kentaro Hirose, Taishi Shiomi, Shunya Hozumi, and Yutaka Kikuchi

BMC Dev Biol. 2014; 14(1): 42.